# HANDHELD IMPEDANCE BASED BIOSENSOR SYSTEM FOR GLUCOSE MONITORING

**Amir Mohsen Aliakbar**

Department of Electrical and Computer Engineering

McGill University, Montreal

August, 2009

A Thesis Submitted to McGill University in Partial Fulfillment of the Requirements of the Degree of

**Master of Engineering**

# ABSTRACT

Biosensors play an important role in various applications including environmental monitoring, food and beverage industry, biomedical/clinical monitoring, and national security. Biosensors are devices or systems that monitor various physical, chemical or biological parameters in the surrounding environment and provide representative signals that can be measured or stored. The rapid developments in semiconductor technologies have sprouted newer integrated sensor technologies leading to the development of biosensor microsystems which offer the advantages of easy to use, point-of-care, low power and low cost. These microsystems allow highly sensitive and rapid detection with low sample volumes in cases of disease epidemics. This thesis focuses on the development of integrated, accurate, rapid and continuous monitoring glucose biosensors.

With growing numbers of aging population and rising obesity rates, chronic diseases continue to be a major health problem in Canada and around the world. For instance, diabetes is a chronic disease which currently affects around 3 million Canadians. The cost of health care for diabetes and its complications amount to about $9 billion a year for Canada. In diabetes, the body either does not produce or ineffectively uses insulin, the hormone which regulates movement of glucose from the blood to the cells. It is generally agreed that the future of diabetes management depends on the success in the development of sensor-based continuous glucose monitoring systems. Although continuous glucose determination is presently available, it has evolved from single glucose determination methodology, which was not primary designed for continuous glucose sensing; hence several aspects of present day glucose sensors are not optimal. Notable shortcomings are

that they are not reagent-less or non-replenishable, and often are multiple enzyme-coupled, which can be complicated and prone to error. Here, the glucose sensing is based on using the genetically re-engineered glucokinese as the recognition element developed by Dr. Mark Trifiro research group in the Department of Medicine at McGill University. Glucokinase is extremely specific, only the D-optical isomer of glucose is a substrate; no other sugars bind to the enzyme with real affinity. Glucokinase exists in the human pancreas where it is believed to actually mediate glucose sensing.

The ultimate goal of the project is to develop an implantable glucose biosensor. It is still a long way from achievement, but as a first prototype, we developed a handheld impedance based biosensor system. The underlying sensing technique is suitable for continuous monitoring which is the main novelty in the thesis. The biosensor consists of an impedance measurement device, microfabricated inter-digitized electrodes incorporated with highly selective glucokinase protein sensitive. The real-time impedance measurement device is based on analog devices AD5933 integrated circuit. The microfabricated inter-digitized electrodes are fabricated using photolithography. The prototype sensor system is tested using different concentration of glucose solutions ranging from 0.5 mM to 7.5mM which is physiologically relevant range.

# RÉSUMÉ

Les biodétecteurs jouent une rôle important dans diverses applications comprenant le contrôle de environnement, le contrôle alimentaire, surveillance biomédicale et clinique, et la sécurité nationale. Les biodétecteurs sont des dispositifs ou des systèmes qui surveillent de divers paramètres physique, chimiques ou biologiques dans l'environnement, et ils fournissent les signaux représentatifs qui peuvent être mesurés ou enregistrées. Les développements rapides en technologies de semi-conducteur ont poussé de plus nouvelles technologies de capteur intégré menant au développement de biodétecteur microsystèmes qui offrent les avantages de facile à employer, point-de-soin, de basse puissance et à prix réduit. Ces microsystèmes permettent la détection fortement sensible et rapide avec de bas volumes témoin dans les cas des épidémies de la maladie. Cette thèse se concentre sur le développement des biodétecteurs integreted qui sont rapide et précise, pour le contrôle continu du glucose.

Avec un vieillissement de la population et le nombre croissant de cas d'obésité, les maladies chroniques continuent à être un problème de santé important au Canada et dans d'autres régions du monde. Par exemple, les diabetes est une maladie chronique qui affecte autour 3 millions de Canadiens. Le coût de santé pour le diabète et ses complications s'élèvent à environ $9 milliards par année pour le Canada. En diabète, le corps ne produit pas ou n'emploie pas inefficacement l'insuline, qui est l'hormone qui règle le mouvement du glucose du sang aux cellules. Il est généralement convenu que le futur de la gestion de diabète dépend du succès dans le développement des systèmes de surveillance continus à base de détecteur de glucose. Bien que la détermination de

glucose continue soit actuellement disponible, il s'est développé de la méthodologie de détermination de glucose simple, qui n'était pas principale conçue pour le détection continu de glucose; de là plusieurs aspects de capteurs de glucose de jour présents ne sont pas optimaux. Les imperfections notables sont qu'elles ne sont pas réactif-moins ou non-replenishable, et sont souvent le multiple enzyme-couplé, qui peut être compliquée et à erreur encline. Ici, la détection de glucose est basée sur employer le glucokinese génétiquement re-machiné comme élément d'identification développé par le groupe de recherche de Dr. Mark Trifiro dans le département de la médecine à l'université de McGill. Glucokinase est extrêmement spécifique, seulement l'isomère D-optique du glucose est un substrat; autre sucre ne lie pas à l'enzyme avec la vraie affinité. Glucokinase existe dans le pancréas humain où on l'est censé agir réellement en tant que médiateur pour la détection de glucose.

Le but final du projet est de développer un biodétecteur implantable de glucose. Il est toujours loin de l'accomplissement, mais comme premier prototype, nous avons développé un système de biodétecteur basé par impédance tenue dans la main. La technique de détection fondamentale convient au contrôle continu qui est la nouveauté principale dans la thèse. Le biodétecteur se compose d'un dispositif de mesure d'impédance avec les électrodes inter-digitalisées fabriqué par microfabrication, les électrodes sont incorporées avec la protéine glucokinase fortement sélective. Le dispositif en temps réel de mesure d'impédance est une circuit intégré basé des unités analogiques AD5933. Les électrodes inter-digitalisées sont fabriqués en utilisant la photolithographie.

Le prototype de la système de détection est examiné en utilisant les solutions de glucose avec concentration différente.

# ACKNOWLEDGEMENTS

I would like to acknowledge and thank my supervisor Prof. Vamsy Chodavarapu for his continual guidance and valuable suggestions throughout my study. I would like to acknowledge the support of Dr. Ebrahim Ghafar-Zadeh, Post-Doctoral Fellow in Sensor Microsystems Laboratory at McGill University, for his support through this thesis. Finally, I would like to thank the members of Prof. Mark Trifiro Research group at the Lady Davis Institute for Medical Research, McGill University, for their contribution towards the development of the Glucokinase proteins and linker chemistry for its immobilization.

# INDEX

ABSTRACT..... ii

RESUME... ..... iv

ACKNOWLADGMENTS... ..... vii

INDEX... ..... viii

LIST OF FIGUERS... ..... xi

LIST OF TABLES... ..... xiii

CHAPTER 1 INTRODUCTION ..... 1

1. Introduction and Motivation... ..... 1

1.1 Biosensors ..... 1

1.1.1 Labeled and Label Free Biosensors ..... 2

1.1.2 Physical Sensing Methods ..... 3

1.1.2.1 Photonic Biosensor ..... 4

1.1.2.2 Thermal Biosensor ..... 4

1.1.2.3 Magnetic and Electrical Biosensors ..... 5

1.2 Glucose Sensing ..... 6

CHAPTER 2 IMPEDANCE BIOSENSING ..... 11

2.1 Impedimetric Biosensor ..... 11

2.1.1 Sensing Electrodes ..... 11

2.1.2 Principle of Impedance Change ..... 12

2.1.2.1 Electrical Modeling ..... 15

2.1.3 Impedance Measurements ..... 16

CHAPTER 3 SENSING PLATFORM ..... 20

3 Overview of Sensing Platform ..... 20
3.1 Microelectrodes Fabrication ..... 20
3.1.1 Sputtering ..... 21
3.1.2 Photolithography ..... 22
3.1.3 Wet Etching Process ..... 23
3.1.4 Packaging ..... 23
3.1.5 Epoxy Capsulation ..... 24
3.2 Glucokinase Immobilization on Electrode ..... 24
3.2.1 Glucokinase Preperation ..... 25
3.2.2 Surface Preperation ..... 25
CHAPTER 4 IMPEDANCE READER ..... 28
4. High Throughput Impedance Reader ..... 28
4.1. Principle ..... 28
4.1.1 Circuit Design ..... 29
4.1.2 Circuit Components ..... 30
4.1.3 AD5933 Evaluation Board Overview ..... 32
4.1.4 Experimental Result ..... 36
4.2 Programming ..... 37
4.2.1 Principle ..... 38
4.2.2 Algorithms ..... 40
4.2.3 Software Modifications ..... 41
CHAPTER 5 Biological Testing results ..... 47

5. Overview Biological Testing Results ..... 47

5.1. Frequency-Domain Measurement..... 47

5.2 Time-Domain Measurements..... 48

6. Conclusion and Future Works ..... 50

LIST OF FIGURES

Figure 1: (a) Immobolized Recogniation Element,(b) label-free analyte in contact with (RE),(c) labeld analyte in Contact with ..... 3

Figure 2: Commercially available Glucose meter ..... 8

Figure 3: Proposed impedimetric sensor platform ..... 9

Figure 4: ECIS ..... 12

Figure 5: Electric field between the Inter-digitized electrode arrays ..... 13

Figure 6: Electric field with recogonation element immoblized ..... 13

Figure 7: Electric field interacting with the immobilized recognition element ..... 14

Figure 8: Electrical model of inter-digitzed biosensor ..... 15

Figure 9: Impedance vs Frequency ..... 18

Figure 10: Impedance vs time at constant frequency ..... 19

Figure 11: Sputtering ..... 21

Figure 12: Spin coating ..... 22

Figure 13: Substrate after development ..... 22

Figure 14: Fabricated inter-digitized electrode ..... 23

Figure 15: Wired bonded inter-digitized electrode ..... 24

Figure 16: Immobolized Glucokinase with all Linkers ..... 25

Figure 17: AFM image of electrode (a)NTA (b) ($Ni^{++}$) (c) immobilized Glucokinase ..... 26

Figure 18: SEM image of immbolized Glucokinase ..... 27

Figure 19: Transition state algorithm ..... 29

Figure 20: Proposed circuit of impedance coder ..... 30

Figure 21: Circuit schematic ..... 31

Figure 22: Final assambeled circuit ..... 32

Figure 23: Block diagram of measurement device ..... 33

Figure 24: Transission block..... 34

Figure 25: Current to Voltage amplifier ..... 34

Figure 26: Electrode arrays..... 37

Figure 27: Experimental test of electrode array..... 37

Figure 28: Analog Devices communication protocols..... 38

Figure 29: Original GUI..... 39

Figure 30: Original software algorithm ..... 40

Figure 31: Modified software algorithm..... 44

Figure 32: Modified GUI..... 45

Figure 33: : Frequency sweep of different concentration of glucose..... 48

Figure 34: Impedance change of Bio-sensing electrode impedance..... 48

Figure 35: Repeatable tests ..... 49

# LIST OF TABLES

Table 1: Output excitation ranges ……..……...33

Table 2: An analog device programmable registers……..41

# CHAPTER 1

# INTRODUCTION

## 1. Introduction and Motivation

Biosensors play an important role in various applications including environmental monitoring, food and beverage industry, biomedical/clinical monitoring, and national security [1]. Biosensors have been used to detect various biological compounds including DNA [2], glucose [3], cholesterol [4], and urea [5]. Biosensors are devices or systems that monitor various physical, chemical or biological parameters in the surrounding environment and provide representative signals that can be measured or stored. The signals provided by the sensors can be used by humans or automated robotic systems to understand, learn, and act upon the environment surrounding the sensors.

Design and fabrication of biological instrumentation in smaller size-scales is an important contribution to the field of health sciences. Portability of biosensors has become very important since in many remote areas where a full-scale biological lab implementation is difficult. Miniaturized biosensors allow rapid and sensitive diagnostic measurement of many diseases. Miniaturization of biosensors opens the path to in-vivo implantation of sensors in the body of patients for unparalleled continuous monitoring.

### 1.1 Biosensor

A biosensor can be defined as a device that consists of a *recognition element* that undergoes a physiochemical change in the presence of an *analyte* (substance to be monitored) and a *transducer* that detects the physiochemical changes in the recognition

element and provides a readable output by converting one type of energy to another. Sensors could be as crude as canary in cage which was used by miner to detect methane gas or as sophisticated as nuclear magnetic resonance (NMR) sensor [6]. The first portable chemical sensor was developed by Hughes in 1922 [7] for pH detection. The first biochemical sensor was developed by Leland Clark in 1954 [8] for oxygen sensing. Since the 1980's, the developments in semiconductor technologies has sprouted newer integrated sensor technologies based on the advances in opto-electronics, electro-mechanics, acoustic-electronics, and microwave/radiowave-electronics. These continued developments have led to exquisite biosensor microsystem technologies for sensing various analytes and diseases including E. Coli [9], hepatitis [10], Salmonella [11] and Bacteria growth [12]. In this section, different sensing techniques and their corresponding systems are discussed.

### 1.1.1 Labeled and Label Free Biosensors

For an affinity biosensor, the recognition element such as protein or phage is immobilized on the surface of biosensor. The recognition element is the biological compound which binds with a specific target analyte. The physio-chemical interaction between the analyte and the recognition element caused by the binding is monitored and measured. By analyzing the signals generated, the concentration of the target analyte can be determined.

Affinity Biosensors are separated into label and label-free Biosensor [13]. In a labeled biosensor the target analyte is attached to a label. During the measurement the amount of signal generated by label in response to the biosensing process is detected. Assuming

direct relation between label concentration and target analyte presence, the concentration of the target analyte can be measured. Labels can be chemical materials such as fluorophores or non-chemical materials such as magnetic beads. In a label-free biosensor, the changes caused directly by the target analyte and recognition element interaction are measured. There are many types of interaction such as hybridization [14] and deformation [15] of recognition element.

Label-free biosensor is preferred over Labeled biosensor because of cost reduction and time required to prepare a labeled target. Also it has been noticed that labeling the target changes the binding property which may result in inaccurate readings [16]. Figure 1 shows a sensing mechanism of labeled and label-free biosensors.

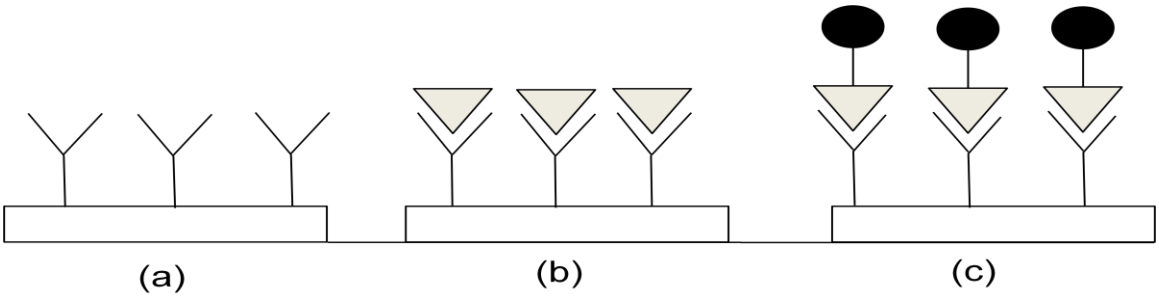


**Figure 1:** (a) Immobilized Recognition Element,(b) label-free analyte in contact with (RE),(c) labeled analyte in Contact with(RE)

### 1.1.2 Physical Sensing Methods

There are several methods to detect the interaction between analyte and recognition element. The detection method could be photonic, thermal, magnetic and electrical.

#### 1.1.2.1 Photonic biosensor

In optical biosensing, the recognition element or the target analyte includes a fluorescent label in most cases. After the target analyte is exposed to the recognition element, the binding process takes place. During this binding event, the recognition element is excited with an electromagnetic radiation of higher energy. The recognition element absorbs the excitation energy and subsequently fluoresces with an electromagnetic radiation of lower energy. The variation in the electromagnetic radiation in response to the interaction between the analyte and fluorophore, mostly in the visible spectrum, is monitored in the form of emission intensity or emission lifetime to provide information regarding the target analyte.

Photonic biosensors have been used refractive index (RI) methods to detect antibody–antigen binding [17] and Listeria bacteria [18]. They have used fluorescence lifetime methods to detect oxygen concentration [19] and bovine serum albumin [20].

#### 1.1.2.2 Thermal biosensor

In thermal biosensors, the recognition element is immobilized on transducers such as quartz chips. The reaction or binding between the analyte and immobilized agent causes a release of chemical energy. This energy release will cause temperature variation on a very small scale. This temperature variation is measured to detect the concentration of the analyte. Thermal biosensors have been used to detect Urea and Glucose [21] by using thin-film thermistors.

#### 1.1.2.3 Magnetic and Electrical Biosensors

Although there are some methods to detect analyte concentration using changes in magnetic flux [22], most of magnetic biosensors are used in conjunction with electrical biosensors to improve detection sensitivity by using magnetic beads as tags to the recognition elements or the target analyte [23]. By applying an external magnetic force, the beads with the target analyte move towards the immobilized recognition element. Magnetic beads can be moved in different directions to interact with various recognition elements in random or in a sequence. The reaction between the analyte on magnetic beads and recognition element is measured by using an electrical biosensor.

Biosensors with electrical read-out measure either current or voltage to detect the binding of analyte and recognition element. There are several different methods that electrical measurements are performed such as voltammetric, amperometric and impedimetric. In Voltammetric and amperometric, DC excitation voltage is used and the resulting current or voltage variation in the solution is measured. However, in impedimetric measurements, AC voltage at different frequencies is used to measure the impedance variations. This method is commonly known as Electrochemical Impedance Spectroscopy (EIS) [24].

Electrical biosensors with conductive electrodes can be separated into faradic and non-faradic sensors. In a faradic biosensor, interaction between recognition element and analyte results in transfer of ions to or from conductive metal electrodes. In non-faradic

biosensors, no transfer of ions takes place and change in the electrode capacitance is due change of dielectric and deformation of recognition element on top of electrode. The changes of dielectric are detected through AC voltage to electrodes. The most important advantage of non-faradic biosensor is that recognition element will not get depleted as in faradic case. The biosensor used in this thesis is non-faradic. Impedance changes in the non-faradic impedimetric biosensor are due to dielectric changes when analyte is introduced on top of electrode. To measure both capacitance and resistance of the test solution containing the analyte, an AC voltage with different frequencies is applied to the electrodes. By plotting the Nyquist plot the capacitance and resistance of analyte can be calculated for different concentrations [25, 26].

There are other Biosensors worth mentioning such as Ion-sensitive Field effect transistors (ISFET) which measure ion concentration in solutions by interaction of surface charges on the gate of a field effect transistor which modulate the charge carrier densities in the transistor. ISFET has been used to detect various analytes including glucose [27].

### 1.2 Glucose Sensing

Glucose is a very important carbohydrate in biology which is used as source of energy by the living cells. With growing numbers of aging population and rising obesity rates, chronic diseases continue to be a major health problem in Canada and around the World. For instance, diabetes is a chronic disease which currently affects about 3 million Canadians and 170 million Worldwide. Diabetes if not treated correctly will cause serious side effects such as heart disease, kidney failure, and blindness. The cost of health

care for diabetes and its complications amount to about $9 billion a year for Canada. In diabetes, the body either does not produce or ineffectively uses insulin, the hormone which regulates movement of glucose from the blood to the cells. Though much effort has been devoted to assure better treatment for diabetes, mostly due to the development of different insulin preparations, treatment centers, and multi-disciplinary team approach, little has changed in most recent times with regards to outcome management. Although a cure for diabetes would be an ideal solution but remains very elusive, thus other options can be considered that can still have a large impact on the course of the disease. A more intense insulin delivery system whose target is to maintain euglycemic (normal blood sugar) control at all times can make a substantial difference, given the fact that diabetic complications are related to glucose control. Perfecting such systems in essence would create an artificial pancreas. The limiting factor here is not the mechanism of insulin delivery, which has been well developed [28, 29], but is the area of glucose sensing. Thus, it is generally agreed that the future of diabetes management depends on the success in the development of sensor-based continuous glucose monitoring systems. Thus, this thesis focuses towards a system for continuous real-time glucose monitoring which can be used for a fully functional artificial pancreas.

There are many commercial glucose detection devices (samples shown in Figure 2) offered by companies such as Abbot and One touch which detect the glucose concentration through electrochemical reaction of glucose oxidase [30].

**Figure 2:** Commercially available glucose meters

In this method, for each measurement a blood sample is taken from the body using a non reusable needle. The blood drop reaches the sensing area where the glucose oxidase reduces to gluconic acid in presence of glucose and is detection through various electrochemical means [31]. The following chemical reaction is used to detect glucose concentration:

$$\text{glucose} + \text{oxygen } (O_2) \xrightarrow{\text{Glucose Oxidase( GOx)}} \text{gluconic acid} + \text{hydrogen peroxide } (H_2O_2)$$

This reaction was first used by Clark and Lyons in 1962 [32], the glucose concentration was measured by the monitoring of oxygen consumed. In this reaction Glucose Oxidase (GOx) was used a catalyst. The glucose reacts with oxygen and produces gluconic acid and hydrogen peroxide. The enzymatic reactions such as the one mentioned, need regents for catalysis to occur; therefore, they require replenishment. The need for GOx to be replenished makes it an unlikely candidate for continuous glucose monitoring. To monitor glucose continuously a regent-less electrode and new sensing techniques are required. In 1973, Guilbault and Lubrano [33] described an enzyme electrode to detect glucose concentration using amperometric method by measuring the current induced by following reaction:

$$H_2O_2 \longrightarrow 2H^+ + O_2 + 2e^-$$

The current commercial systems use hydrogen peroxide oxidation to measure the glucose in the blood sample. Although the method has been developed and widely used for over 30 years and has become accurate, there are some limitations with this method. For instance, glucose oxidase responds to all sugars and not just glucose.

In order to have a continuous monitoring of glucose a regent-less sensing technique is required. The Figure 3 presents an impedimetric biosensor suitable for continuous real time glucose monitoring. This setup consists of protein coated electrodes, impedance measurement device and a read-out interface.

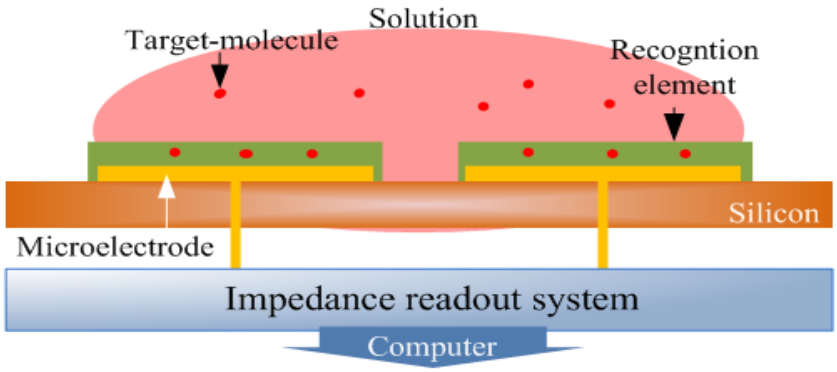


**Figure 3:** Proposed impedimetric sensor platform

The developed prototype sensor is based on using glucokinase as the recognition element which is extremely specific to glucose, only the D optical isomer of glucose is a substrate; no other sugars bind to the enzyme with real affinity. Glucokinase has a glucose affinity constant of 5 mM, which is very physiological, and exists in the pancreas where it is believed to actually mediate glucose sensing. Glucokinase protein has been extracted through biological assays and can be immobilized on top of metal microelectrodes [34-35]. Glucokinase protein has been genetically engineered by Dr.

Mark Trifiro research group at the Lady Davis Institute for Medical Research (LDIMR), McGill University [36]. The physiochemical changes caused by glucokinase and glucose reaction are measured through an impedimetric technique. The initial concept behind this method has been demonstrated by Trifiro et al. [37].

Impedance measurement has been used for many applications such as detecting DNA [38], virus [39], and glucose [40]. However, the previous implementations used bulky table top systems. In this thesis, a handheld scale impedance reader system is developed based on analog devices AD5933 integrated circuit. Real-time continuous glucose sensing is a first step toward designing implantable artificial pancreas.

# CHAPTER 2

## IMPEDANCE BIOSENSING

### 2.1 Impedimetric Biosensor

In this section, impedimetric biosensing technique is more thoroughly discussed. First, the sensing electrode configuration and sensing material are discussed. Second, their impact on the sensitivity and selectivity of impedimetric biosensor is discussed. Finally, the electrical model to characterize the change in impedance is presented.

#### 2.1.1 Sensing electrodes

Sensing electrodes have direct interaction with the analyte and test solutions. Therefore, the material and geometry of electrode have direct impact on the impedance measured. Also, the material used for fabrication and configuration of the electrode plays an important role in the sensitivity and biocompatibility. The immobilization of the recognition elements is sensitive to the material used for fabrication of electrodes. Most of the recognition elements can be coated only on a specific type of material such as gold. Complex and expensive chemical processes have to be performed to coat a recognition element on a non-suitable material; therefore, it is important to know which material can bind with the selected recognition element prior to fabricating the electrodes. Gold is a noble metal and is compatible with most immobilization strategies and is selected for the work in this thesis.

There are various shapes and configurations available for the sensing electrode such as inter-digitized, half circle, half plane, etc. The shape and size of the electrode has a direct

relation to the resulting electric fields and sensitivity of the electrode which will be discussed in the following Sections. Also, we prefer low-cost disposable electrodes for easy of use such as screen printed carbon electrodes which have been used for glucose monitoring [36]. Some biosensor electrodes are also currently commercially available. Figure 4 presents one of commercially available electrodes from Applied BioPhysics Inc [41].

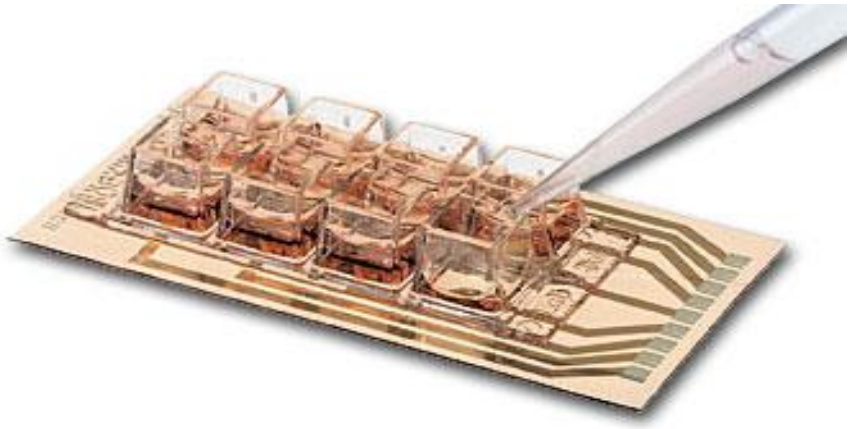

**Figure 4:** ECIS [41]

In this thesis, inter-digitized microelectrode arrays are used. Inter-digitized microelectrodes arrays have shown to improve sensitivity compared to other configurations [42]. Inter-digitized electrodes configuration have been used in biosensor applications to detect Urea [43] and IgG [44].. The fabrication process for the inter-digitized electrodes is discussed in the next Chapter.

### 2.1.2 Principle of Impedance Change

In impedimetric biosensor, the binding between recognition and biomaterial occurs above the surface of electrodes; this change is scanned by electrode electric field which results

in an impedance change. The electrode array and the corresponding electric fields are shown in Figure 5.

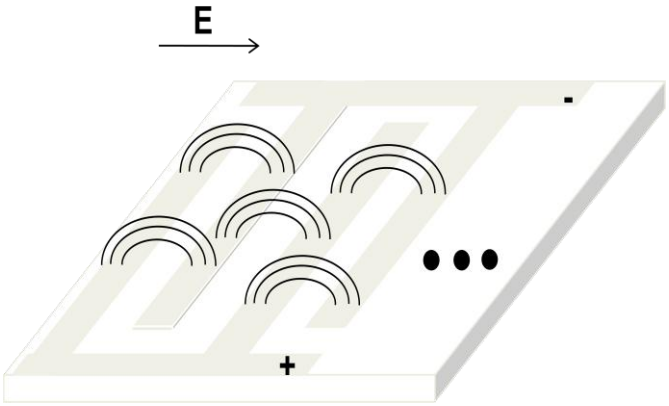


**Figure 5:** Electric field between the Inter-digitized electrode arrays

The recognition element is immobilized on top of the electrode. Figure 6 depicts the immobilized recognition element on top of the electrode and the interacting electric field.

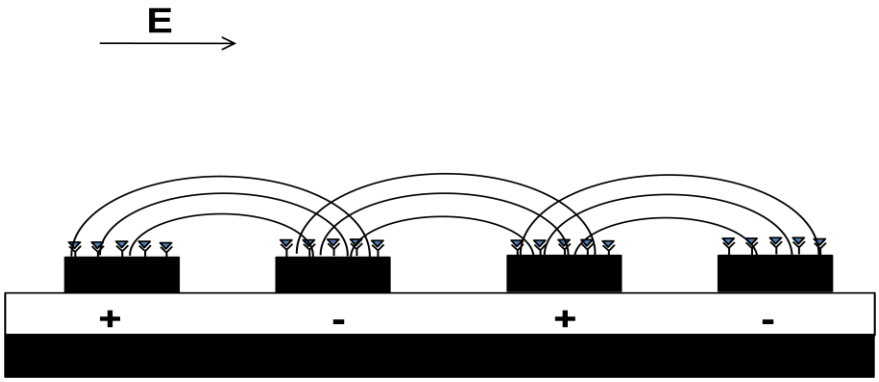


**Figure 6:** Electric field with recognition element immobilized

The electric field on top of electrode has an inverse relation to the distance from the electrode. The Laplace equation $\nabla^2\varphi = 0$ is used to calculate the value and maximum distance of electric field penetration. The Laplace equation is solved using the boundary values. After some calculation, electric field at point x and y above the electrode (Figure 7) could be derived from the following equation [42].

$$\Phi(x, y) = \frac{V}{2K(\sin\frac{\pi Wsp}{2L})}\mathrm{Re}\left(F\left(A\sin\left(\frac{\sin(\pi(\frac{x+iy}{L})}{\sin(\frac{\pi wsp}{2L})}\right), \frac{\pi wsp}{2L}\right)\right) \quad (1)$$

where, V is the voltage between electrodes, K (k) is complete elliptical integral of with modulus k, F (α , β ) is an incomplete elliptical integral which α is amplitude and β is modular angle [45]. Assuming the spacing between the electrode (Wsp) and their width (Wel) is equal and the voltage is applied differentially as ($-\frac{V}{2}, \frac{V}{2}$ ), the result of equation can be demonstrated in Figure 7.

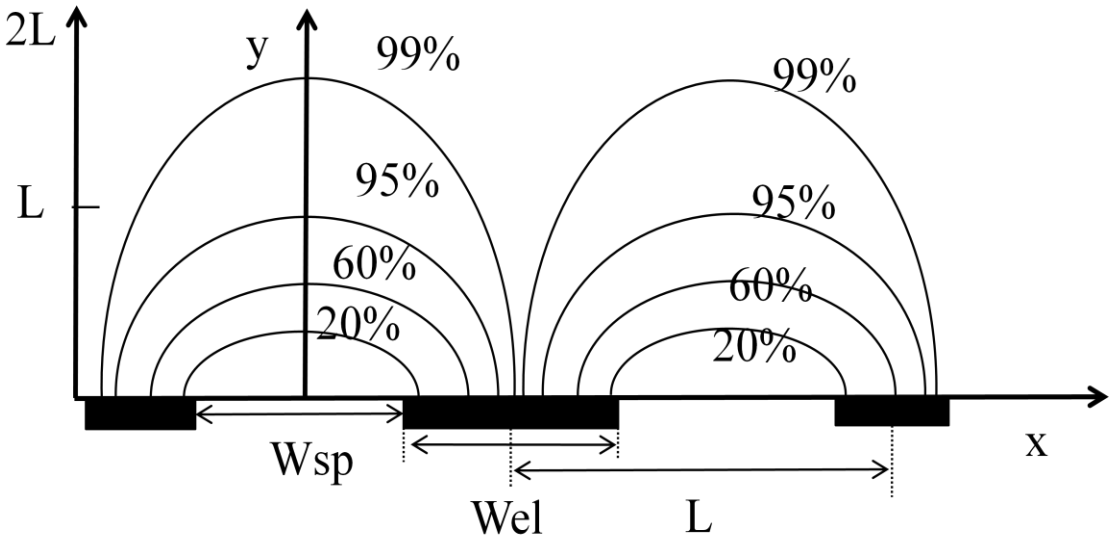


**Figure 7:** Electric field interacting with the immobilized recognition element

The impedance is calculated using a ratio of voltage over current. The current change in the inter-digitized electrodes is due changes of dielectric medium above the electrode. Figure 7 represents the percentage of current in the electrodes due to the electric field. It

is clear from the graph that up to 99% of change in current happens with in a distance 1.6 L which means any change in dielectric above 1.6L will have minimal effect on the current measured in the electrodes. Space between 0.4L and 1.6L contribute only 4% to current change; therefore it is safe to assume that electrode field penetration and sensitivity of the electrode is at 0.4L above the electrodes.

For this thesis 100 µm and 50µm electrode with equal spacing were used; therefore 95% of current change occurs in a distance no higher than 40µm and 20µm. The immobilized recognition element has a height which is less than 1µm (see Figure 17) so the changes will be monitored by the electric field above the electrode.

#### 2.1.2.1 Electrical Modeling

The total capacitance and resistance due to analyte introduction on top of electrode has to be modeled. Electrical modeling provided in this section is for a non-faradic biosensor. The impedance between two non-faradic electrodes can be modeled with different models; however, the one commonly used for non-faradic biosensor is presented in Figure 8.

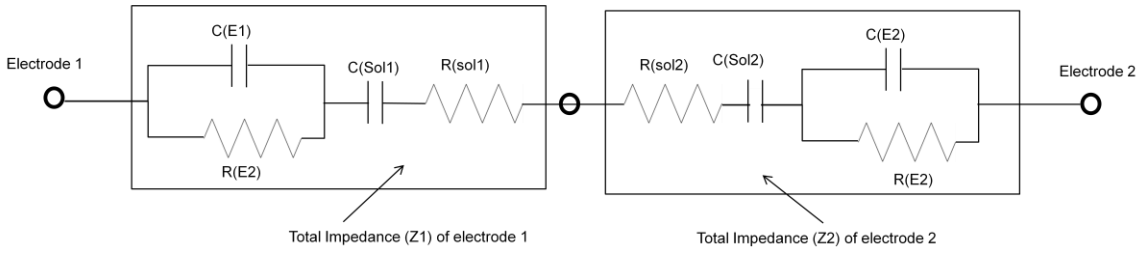


**Figure 8:** Electrical model of inter-digitized biosensor

$C_{E1}$ and $C_{E2}$ are total capacitance of electrode 1 and electrode 2, respectively. These capacitances are due to binding analyte to the immobilized layer and double layer

capacitance on top of each electrode. Double layer capacitance is due positioning of solution ions above the binding site. Although analyte molecules may be neutral, they will have charge cloud distribution on their molecular structures. Once target analyte binds with immobilized layer, positive or negative ions from the solution will accumulate of top of target due to molecular charge clouds. $R_{sol}$, $C_{sol}$ are solution resistance and capacitance.. $R_{sol}$ and $C_{sol}$ is separated into two resistances $R_{sol1}$ and $R_{sol2}$ and two capacitance $C_{sol1}$ and $C_{sol1}$ to make impedance calculation easier and symmetrical for both electrodes. $R_{E1}$ and $R_{E2}$ represent the charge transfer resistance of electrode 1 and electrode 2 through the immobilized recognition element. This model is not as detailed as described in some other models which can be studied for further details [46].

### 2.1.3 Impedance Measurements

AC voltage is applied and impedance change in biosensor is monitored before and after introducing the analyte on top of electrode through. Impedance measurements obtained are analyzed using Bode and Nyquist plots which provides information about electrical modeling of the electrode and the sample. Measuring the impedance change over time is important because it provides an estimation of response time and other transition issues which are very important for continuous-time monitoring applications.

In this section, we provide the principle and formulas for impedance measurement and provide a simple calculation of the impedimetric electrical model. In Chapter 3, we describe the proposed handheld measurement system which can efficiently be employed for both frequency and time domain analysis. The electrical Model of impedimetric biosensor includes both capacitance and resistance. The value of the capacitance varies

with frequency and is calculated by the following formula:

$$Z(j\omega) = \frac{1}{j\omega C} \qquad (2)$$

where, C is the capacitance value and ω is angular frequency is directly proportional to the frequency f:

$\omega = 2\pi \times f$ (3)

*j* is the complex indicator which indicates the capacitance causes a lag in resulting current by $\pi/2$. The resistance magnitude doesn't change with the frequency; however it will effect in the final value of impedance calculated as follows:

The impedance of electrode 1 ,$Z_1$ is calculated:

$$Z_1(j\omega) = (R_{sol1} + \frac{R_{E1}}{1-(\omega C_{E1} R_{E1})^2}) + j(\frac{1}{\omega C_{sol1}} - \frac{\omega C_{E1} R_{E1}^2}{1-(\omega C_{E1} R_{E1})^2}) \quad (4)$$

The impedance of electrode 2, $Z_2$ is calculated:

$$Z_2(j\omega) = (R_{sol2} + \frac{R_{E2}}{1-(\omega C_{E2} R_{E2})^2}) + j(\frac{1}{\omega C_{sol2}} - \frac{\omega C_{E2} R_{E2}^2}{1-(\omega C_{E2} R_{E2})^2}) \quad (5)$$

Total impedance is $Z_1 + Z_2$ . By replacing $R_{sol1} + R_{sol2}$ with $R_{sol}$ impedance calculated as:

$$Z(j\omega) = (R_{sol} + \frac{R_{E1}}{1-(\omega C_{E1} R_{E1})^2} + \frac{R_{E2}}{1-(\omega C_{E2} R_{E2})^2}) + j(\frac{\omega C_{sol}}{\omega^2 C_{sol1v} C_{sol2}} - \frac{\omega C_{E1} R_{E1}^2}{1-(\omega C_{E1} R_{E1})^2} - \frac{\omega C_{E2} R_{E2}^2}{1-(\omega C_{E2} R_{E2})^2}) \quad (6)$$

The magnitude of complex number is calculated by the following formula:

$$\Rightarrow Z(j\omega) = \sqrt{\mathrm{Re}al^2 + (imaginary)^2} \qquad (7)$$

The Magnitude of total impedance is calculated as:

$$\Rightarrow Z(j\omega) = \sqrt{(R_{sol} + \frac{R_{E1}}{1-(\omega C_{E1} R_{E1})^2} + \frac{R_{E2}}{1-(\omega C_{E2} R_{E2})^2})^2 + (\frac{\omega C_{sol}}{\omega^2 C_{sol1v} C_{sol2}} - \frac{\omega C_{E1} R_{E1}^2}{1-(\omega C_{E1} R_{E1})^2} - \frac{\omega C_{E2} R_{E2}^2}{1-(\omega C_{E2} R_{E2})^2})^2} \quad (8)$$

The measured magnitude vs frequency according to the above results is shown in Figure 9 .

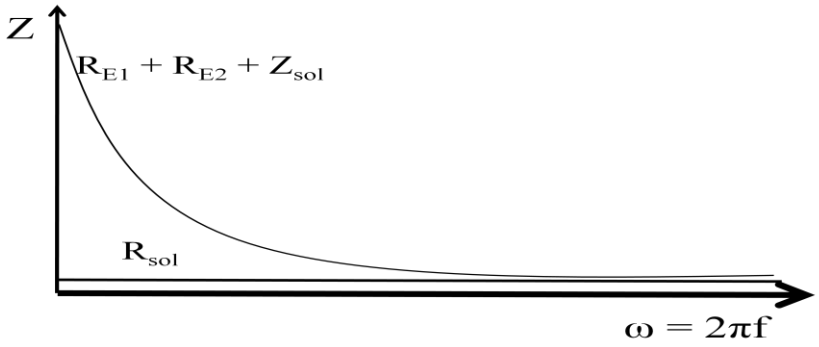


**Figure 9:** Impedance vs Frequency

According to this model, at very high frequencies, the capacitance will act as a short circuit and the total impedance will be equal to $R_{sol}$. However, at low frequencies, the contribution of capacitance to the impedance magnitude is noticable and impedance is equal to $Z_{sol} + R_{E1} + R_{E2}$. Typically, EIS requires a wide range of frequencies to detect the impedance change.

Impedance measurement of biosensors could also be done on certain frequency and over a period of time. In this measurement, a specific frequency is applied to the electrodes and the impedance change is monitored before and after the analyte is introduced on the electrodes. The impedance change could be gradual or sudden depending how fast the binding reaction occurs. Figure 10 presents a sample impedance graph of this type of measurement before and after the analyte is introduced to the solution.

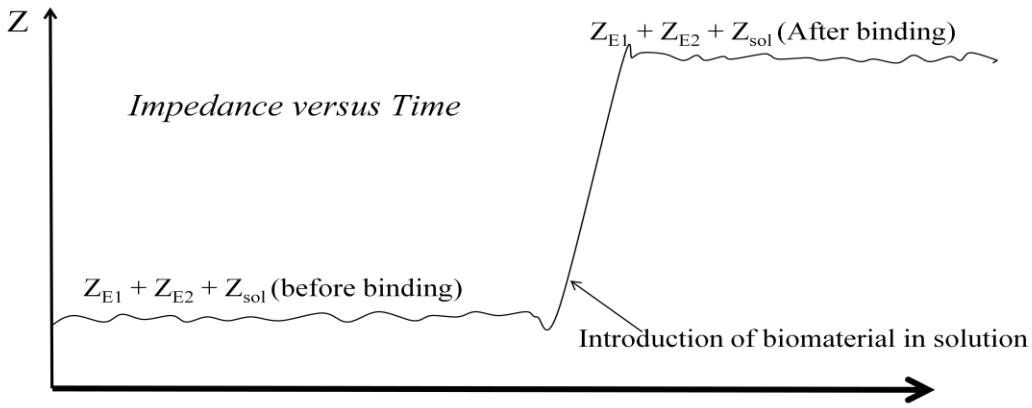


**Figure 10:** Impedance vs time at constant frequency

Impedance measurement systems utilize several different algorithms to measure the phase and magnitude of impedance. The device which is used in this thesis uses Digital Fourier transforms (DFT) for impedance measurement. Brief description of the functionality is provided in following Chapters.

# CHAPTER 3

## SENSING PLATFORM

### 3. Overview of Sensing Platform

The platform developed in this thesis for detecting glucose concentration is by using genetically engineered glucokinase protein. The sensing platform used consists of microelectrodes, glucokinase recognition element and an impedance sensing device. In this chapter microelectrodes and recognition elements are described in detail. The measurement device is described in detail in Chapter 4.

### 3.1 Microelectrodes Fabrication

Microelectrodes form the substrate for immobilization of receptor molecules that bind the target analyte. This section presents different electrode fabrication processes and the process suitable for this application is described.

The electrodes previously used by Dr. Trifiro research group to demonstrate that glucose can be detected using glucokinase were screen printed carbon electrodes [36]. The eight carbon electrodes used were 15mmx25mm in total size and each with a surface of 780 $\mu m^2$. In screen printing method, a modified printer cartridge is used to inject and pattern material on the substrate. The procedure is low cost and fast; however, it has limited resolution and feature size in 100's of microns. Screen printing also limits the type of materials that can be used for the procedure.

To date, different type of sensing electrodes have been used in biosensors such as inter-digitized gold electrodes [47], carbon nanotubes [48], and Ag/Agcl electrodes [49]. Among these electrodes, the focus of this thesis will be on gold electrode fabricated through microfabrication techniques. The electrodes were fabricated using sputtering process by depositing a thin layer of gold and using photolithography and wet etching to pattern the gold layer. Finally, epoxy capsulation has been used to package the electrodes. The electrodes have been fabricated using McGill Clean room facilities.

### 3.1.1 Sputtering

The electrodes are fabricated on top of silicon wafers. The first step of fabrication is deposition of gold on the silicon wafer. It is well known that gold and silicon do not have good adhesion; therefore, an intermediate adhesive layer is needed. . Here, titanium (TI) was used intermediate adhesive layer between silicon and gold. In thin film sputtering argon gas is infused in a closed high vacuum chamber where a plasma in struck. Material and substrate are separated on top and bottom of chamber. Voltage is applied to the target material and substrate is connected to the ground.

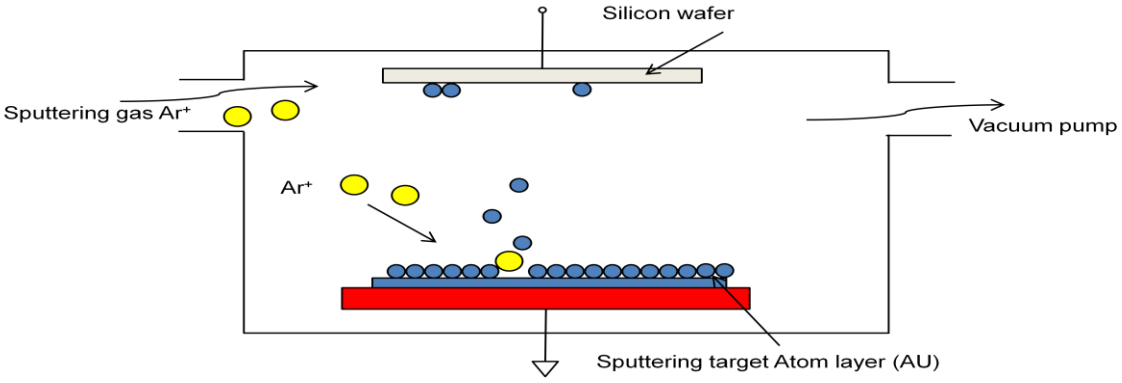


**Figure 11:** Sputtering

Plasma accelerates the argon and collision of argon atoms with the material will remove a thin layer from the material and deposit it on the sample substrate. A Denton Explorer14 sputtering machine was used to sputter 20nm Titanium and 100nm of gold.

### 3.1.2 Photolithography

The Sputtered gold is patterned by using the photolithography. A photoresist layer is spin coated on top of sputtered gold as shown in Figure 12.

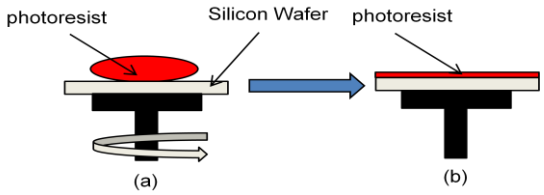


**Figure 12:** spin coating

The four main steps to pattern the metal is, exposing photo resist to ultra-violet light, developing the photo resist, wet etching and resist removal. The photolithography steps needed to pattern the gold is demonstrated in Figure 13.

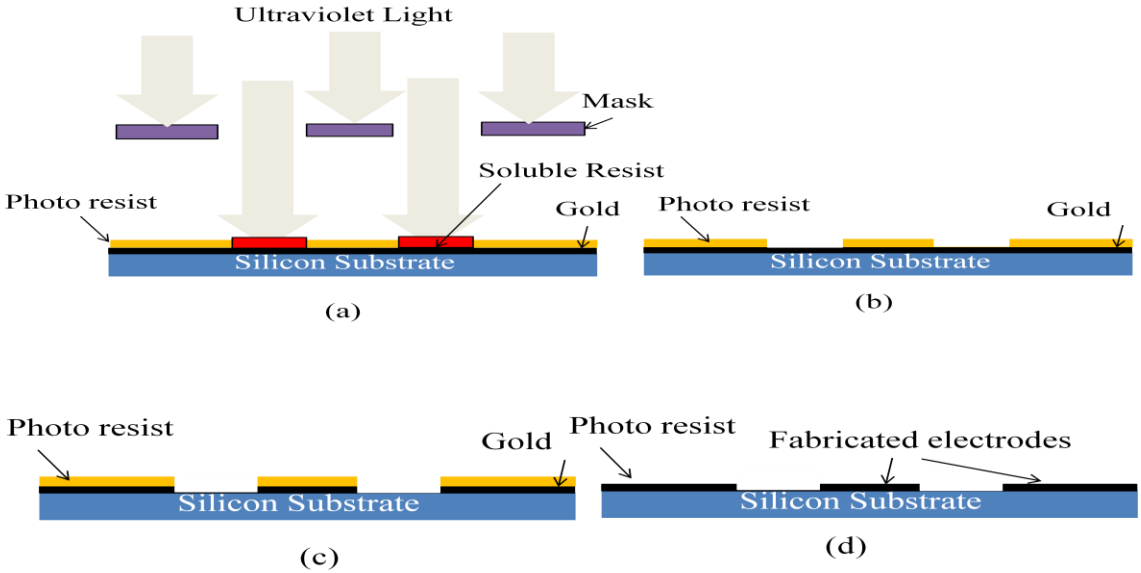


**Figure 13:** Substrate after development

### 3.1.3 Wet etching process

In wet etching, first potassium-iodide (KI) based solution is used to etch the exposed portions of the gold metal film. Then, hydrofluoric acid (HF) is used to etch the Titanium by submerging the sample in HF for 15-30 seconds. Finally, the photo resist has to be removed using acetone. The final device is gold inter-digitized electrodes on top of silicon substrate as shown in Figure 14.

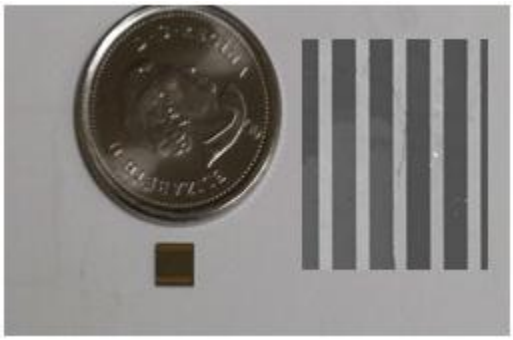

**Figure 14:** Fabricated inter-digitized electrode

### 3.1.4 Packaging

In order to obtain measurements from the electrode, a conductive connection between microelectrodes and measurement system is required. A printed circuit board (PCB) based packaging is low cost and convenient. The PCB is then connected through regular wire-bonding to the measurement device. After wire bonding is completed, an epoxy capsulation is used to cover all the wire bonding and the electrical traces on the PCB. This is necessary to avoid short circuit caused by liquid test samples. The resulting electrode is shown in Figure.15.

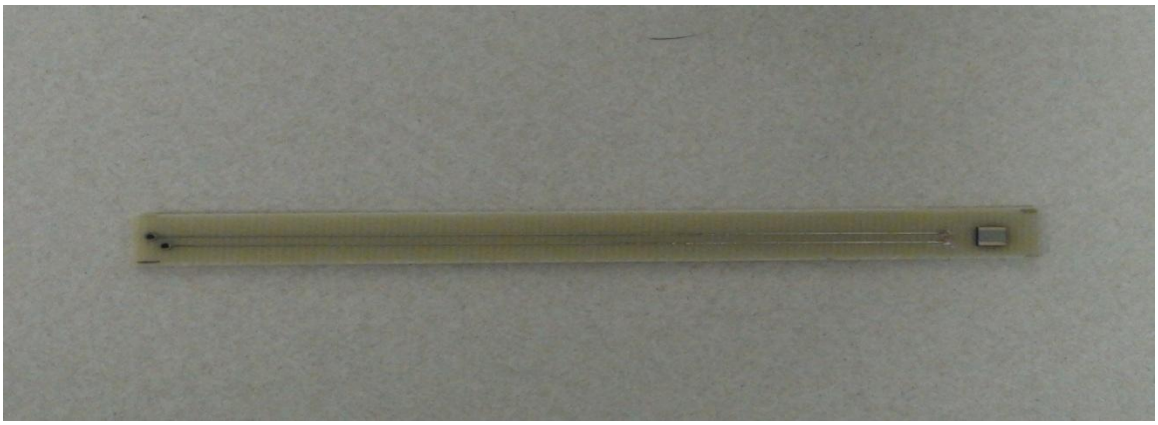

**Figure 15:** Wired bonded inter-digitized electrode

.

### 3.1.5 Epoxy Capsulation

To encapsulate the electrode with epoxy, direct-write fabrication process (DWFP) was used. This process has been previously used to make microfluid channels on CMOS integrated circuits [50]. In this method, an air dispensing robotic deposition device is used to deposit an organic ink on top part of the electrode. After the ink deposition on the PCB, epoxy is deposited. After the epoxy is cured at room temperature for 20-24 hours, the sample is heated to remove the ink from the top of electrode leaving behind the finished sample.

## 3.2 Glucokinase Immobilization on electrodes

As mentioned earlier, the recognition element used for glucose monitoring in this thesis is glucokinase (GLK). To have a strong and stable bond between the immobilized GLK protein and the surface of gold electrodes special linkers are needed. To add the linkers, the gold surface and GLK have to be biochemically prepared. GLK is tagged 6-histine tail (His-tag) and gold electrodes surface are covered by nickel cations ($Ni^{++}$). The

specificity of $Ni^{++}$ and His-tagged GLK proteins is used to immobilize the proteins by exposing the surface treated electrodes to GLK proteins. The final binding configuration is shown in Figure 16.

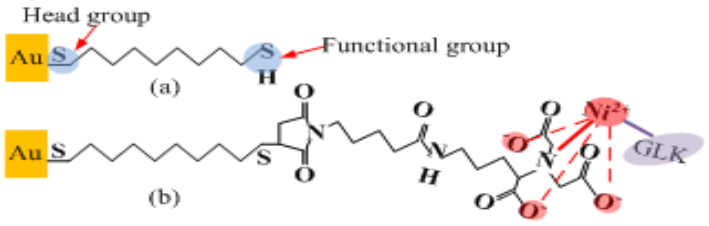


**Figure 16:** Immobilized Glucokinase with all the linkers

### 3.2.1 Glucokinase preparation

Wild type glucokinase can be extracted from human liver. Wild GLK is purified using several biological protocols. In order to use wild GLK as recognition element for sensing glucose, it is genetically re-engineered [37, 51]. Wild GLK has two binding sites [51, 21]. One site is for ATP and magnesium binding and the second site binds with glucose [51, 52]. Through genetic engineering, GLK losses its enzymatic reaction and its binding site with ATP and magnesium.

### 3.2.2 Surface preparation

The gold electrode surface has to be prepared in such way so that the tagged GLK proteins could be immobilized. As mentioned earlier, tagged Glucokinase can be attached to nickel cations ($Ni^{++}$). In order to cover the gold electrodes by nickel cations ($Ni^{++}$), the following biochemical procedures were performed.

A 3:1 mixture of $H_2SO_4$ and 33% $H_2O_2$ was used to remove unwanted residues from the electrodes and electrodes were rinsed with ethanol and di-ionized water. Next, the electrodes were dried with nitrogen gas and then immersed overnight in a 1mM ethanol solution to create a self assembled monolayers (SAM) of 1,8-octanedithiol on top of the electrode. The SAM coated electrode were rinsed with ethanol to remove any physioabsorbed material. Next, SAM coated electrodes were immersed in 10 mM solution of maleimide-C3-NTA (pH 8.5 in Tris–HCl buffer) overnight, in order to perform the coupling reaction of maleimide-C3-NTA and a sulfhydryl surface. NTA ligand electrodes were rinsed by di-ionized water and methanol. An AFM image of electrode after this phase is shown in Figure 17a.

After the electrodes were covered by NTA, NTA ligand electrodes are immersed into 200 mM $NiCl_2$ in order to cover the top by nickel cations ($Ni^{++}$). The electrodes were rinsed with di-ionized water. The electrodes surface with nickel cations (($Ni^{++}$) on top is shown in Figure 17(b). Finally, His-tagged GLK proteins were coordinated on top of electrodes by immersing the electrodes in 100 mM of His-tagged Glucokinase. The electrodes were rinsed with di-ionized water and preserved in a buffer solution. The AFM image of immobilized Glucokinase is shown in Figure 17 (c).

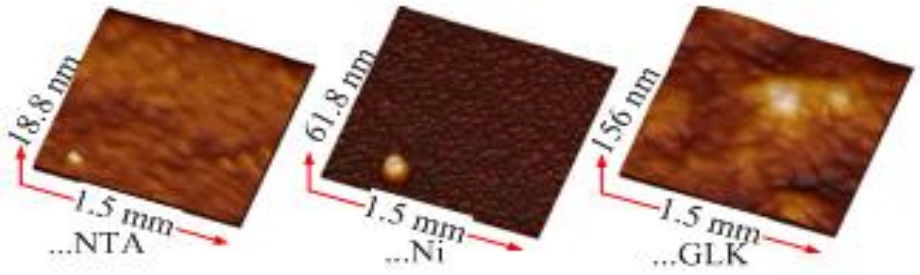


**Figure 17:** AFM image of electrode **(**a)NTA (b) ($Ni^{++}$) (c) immobilized Glucokinase

It can be observed from the AFM image that based on surface morphologies the thickness of sensing probe increases after applying each step. SEM image of the final sensing electrode with immobilized Glucokinase on top is shown in Figure 18.

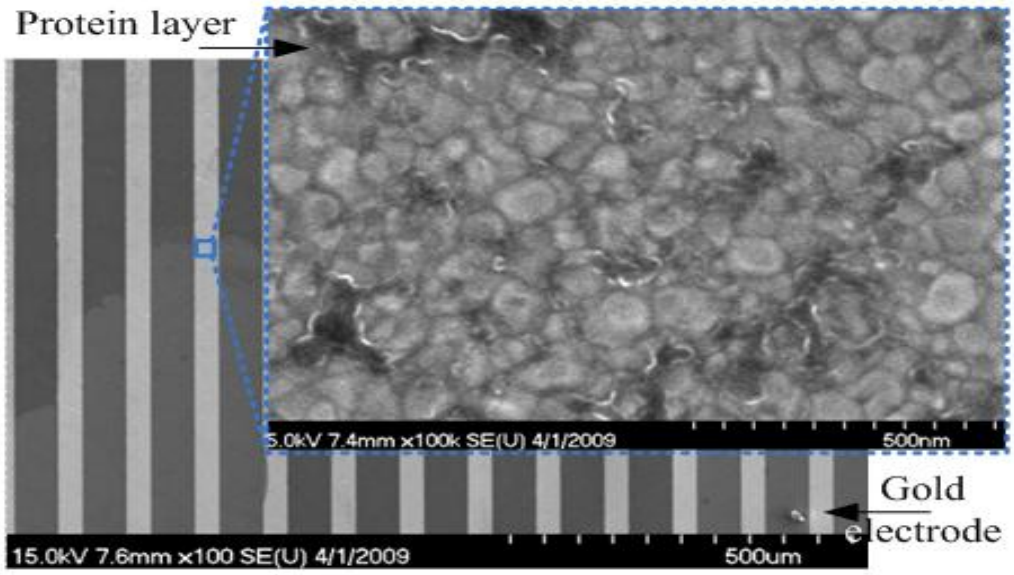


**Figure 18:**SEM image of immobilized Glucokinase

# CHAPTER 4

## IMPEDANCE READER

### 4. High Throughput Impedance Reader System

The proposed impedance system consists of a commercially available point impedance reader, an impedance coder and an impedance decoder. An impedance reader measures the impedance variation of a single electrode and transfers the values as readable data to a computer. An impedance coder is a microelectronic system dedicated to read the impedance values of a large array of sensing electrodes. An impedance coder adds special codes to the impedance signal in order to indentify the location of the sensing electrode in the array. Impedance measurements with special codes attached are processed by impedance decoder algorithm to distinguish between each electrode in the array.

There are several commercially available electronic devices, such as USB-6281 made by National Instruments, which can be used as a single point impedance reader. In this thesis, the AD5933 from Analog Devices was used because of its low cost and user-friendliness. The AD5933 has already been used for health monitoring and single cell analysis [52, 53]. In this chapter, software and hardware modifications used to develop a real-time impedance measurement device are described.

### 4.1 Principle

When a measurement of an array of samples or electrodes is needed, there are two ways to measure impedance change over time. We could individually connect to each of the electrodes to a single-input impedance measurement system (SIMS) or we could use

multiplexing to switch between samples and continuously record the results. To separate each sample in the array, a feedback signal is needed to indicate which sample is being measured. The feedback signal has to be implemented using circuit or clock synchronization. By using clock synchronization, the needed circuitry becomes complex and expensive. The other method to separate and distinguish the samples in the array is to make a transition state between each sample as shown in Figure 19.

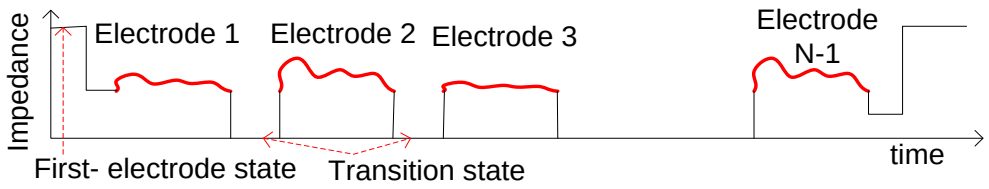


**Figure 19:** Transition state algorithm

While results are being obtained continuously during a period time, a transitions state is setup between each sample. The results are then processed to detect the transition state and samples are separated with computer algorithms to distinguish this transition states and the impedance measurements from each electrode can be detected and separated.

### 4.1.1 Circuit Design

To make the transition state, the circuit as shown in Figure 20 has been designed and assembled on a PCB. Some form of multiplexing is needed to connect the array of electrodes with the measurement system. In order to switch and measure between samples while using SIMS, a clock generator and a counter is used to activate switches s1, s2… in sequence. When each switch is activated a specific electrode connected. In order to distinguish between electrode E1, E2 ,… transitions states are used. The

transition states are implemented by making s1 connected as open circuit, switch s2 will be connected to electrode 1, E1 and switch s3 will be short circuited, s4 will be connected to electrode 2, E2 and so on. The transitions are clear and can be easily separated using a pre-programmed algorithm.

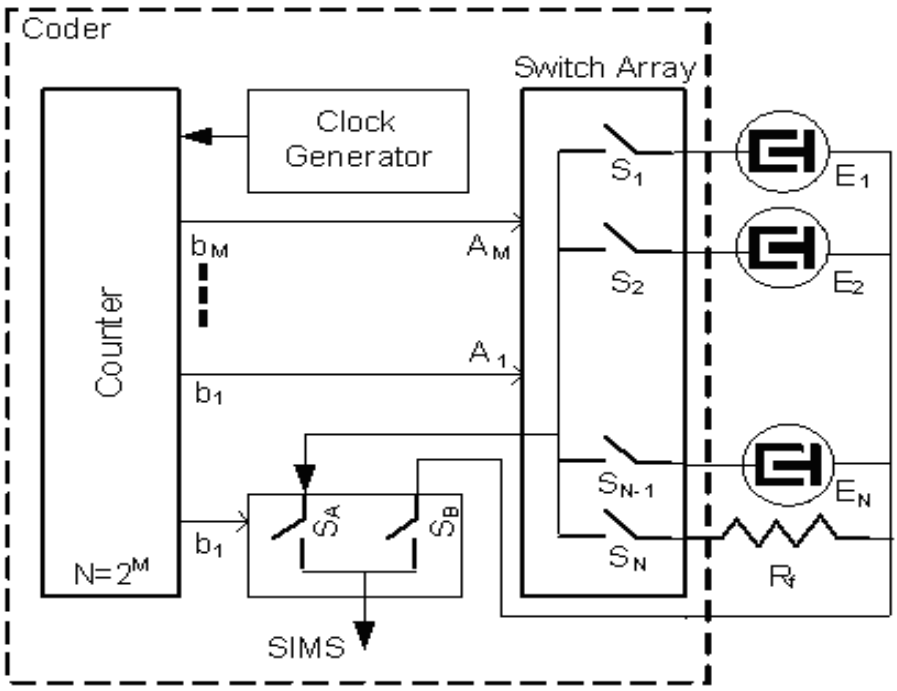


**Figure 20:** Proposed circuit of impedance coder

### 4.1.2 Circuit Components

The proposed circuit which has been implemented on a 10 electrode array consists of a clock generator, counter and 10 switches connected to the electrode and analog devices AD59333. This system is shown in Figure 21. The clock generates the pulses with a frequency less than the recording frequency of SIMS. Pulses generated by the clock activate bits ($B_1$,…$B_M$) in sequence which in turn establish the connection with each

electrode to the SIMS. The chips used in this design are NE555 precision Timer as pulse generator, 74HC4017 Decade Counter with 10 outputs and 3 CD4016BC Quad Bilateral Switches connected to the electrodes. In order to demonstrate functionality of the setup, a PCB board was used to mount the chips. The fully assembled circuit is shown the in Figure 22.

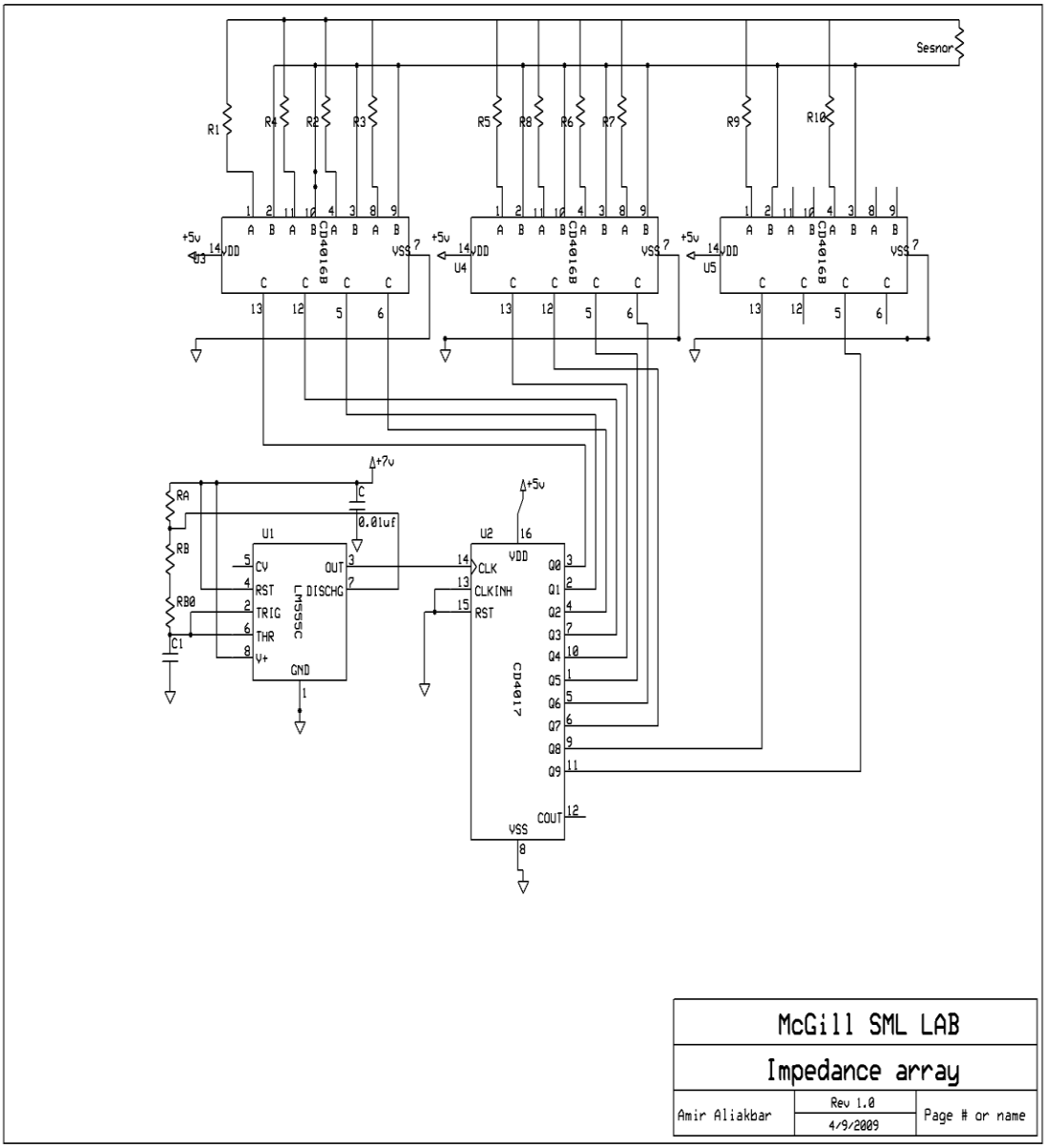


**Figure 21:** circuit schematic

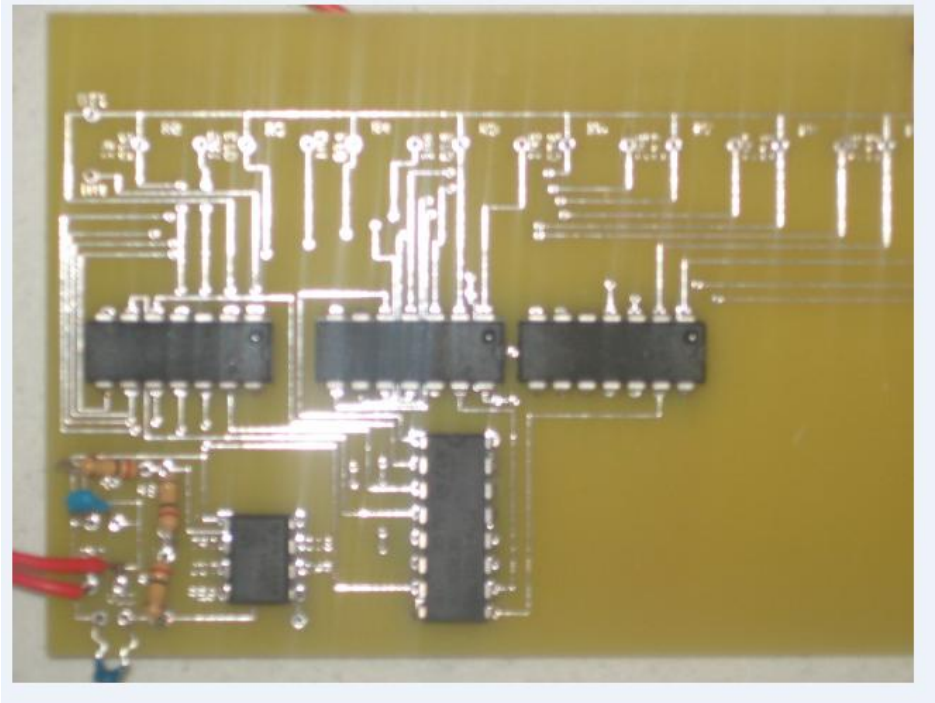

**Figure 22:** Final assembled circuit

### 4.1.3 AD5933 Evaluation Board Overview

AD5933, developed by Analog devices, is a two-electrode high precision impedance measurement device composed of several blocks including a wave generator, an Analog-to-Digital Converter (ADC), an output voltage source, and a Fourier Transform based impedance estimator. It has a dynamic range of 1KΩ to 1MΩ which according to AD5933 datasheet is determined by a variable resistor connected to the input Feedback Resistor ($R_{FB}$). The AD9533 has a maximum frequency of 100 kHz. The operational circuit diagram of AD5933 is shown in Figure 23.

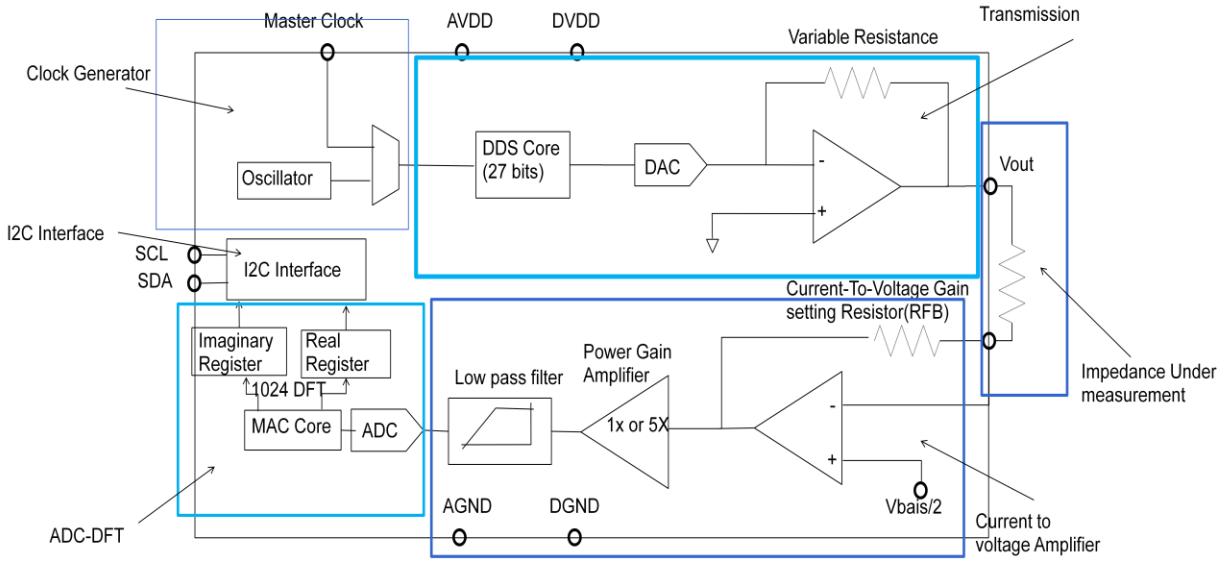


**Figure 23:** Block diagram of measurement device

To measure an unknown impedance Z(ω) which is connected between the $V_{out}$ and $V_{IN}$ terminal of AD5933, a sinusoidal voltage is first used to excite Z(ω). The sine wave is digitally generated by a 27-bit Direct Digital Synthesizer (DDS) with the clock input of the synthesizer provided either by an external clock through a USB connection or internal clock. The generated wavefrom is then amplified through a programmable gain amplifier. Four output excitation voltages are generated through this method. The output voltages are generated by setting the control register of programmable gain stage. The peak-to-peak and DC bias estimates of output voltages are shown in the Table.1.

| **Amplitude of excitation voltage** | **Output DC bias** |
|---|---|
| Range 1:2 $V_{p-p}$ | 1.5 V |
| Range 2:1 $V_{p-p}$ | 0.75 V |
| Range 3:0.4 $V_{p-p}$ | 0.3 V |
| Range 4:0.2 $V_{p-p}$ | 0.18 V |

**Table.1:** Output excitation ranges

The block responsible for generating and applying the excitation voltage to the load is known as transmission block and is shown in Figure 24.

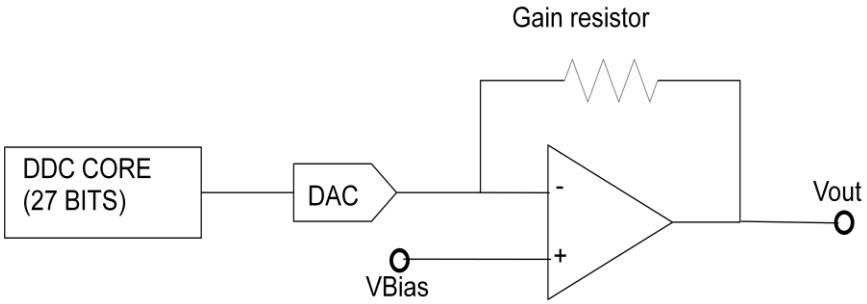


**Figure 24:** Transmission block

After the output excitation voltage is generated and applied to the unknown impedance, the resulting current is acquired and measured. The current is measured by using a current-to-voltage converter. The gain of current-to-voltage converter can be changed by varying the $R_{FB}$ resistance. The resulting voltage is amplified using a programmable gain amplifier (PGA) by setting the gain to either 5 or 1. As demonstrated in Figure 25, the output of the PGA is the input of the ADC.

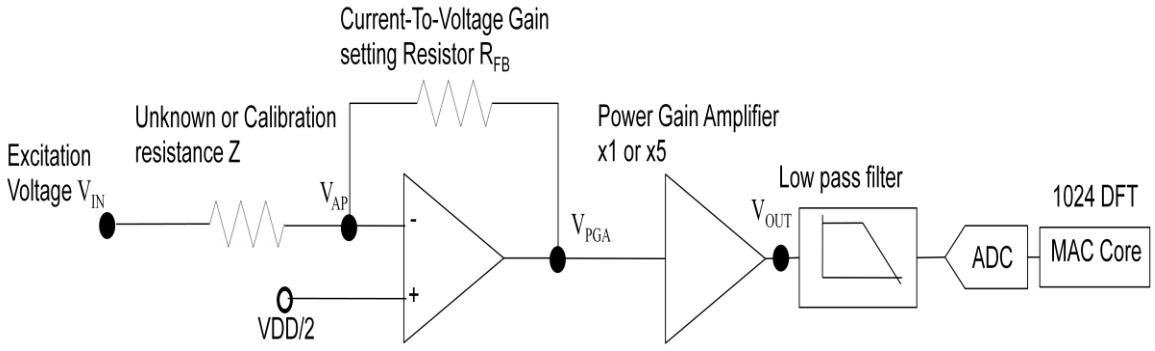


**Figure 25:** Current to Voltage amplifier

Since the maximum sampling voltage of the ADC is 2 V, any voltage input greater than 2V will cause saturation and result in inaccurate measurements. Final value of voltage at PGA output is calculated as follows:

Writing the KCL for the op-amp: $\frac{Vin - Vap}{Z} = \frac{Vap - Vpga}{Rfb}$ (9)

AC gain through Op-Amp is $Vpga = \frac{-Vin}{Z} X (Rfb)$ (10)

Finally, the $V_{out}$ will be: $\frac{-Vin}{Z} \times (Rfb) \times GAIN(pga)$ (11)

It is clear from the calculation that both $R_{FB}$ and PGA gain has to be set correctly to avoid ADC saturation.

In the final stage of impedance calculation, the digital data provided by the ADC are processed by an on-board DSP. The impedance can be calculated by using Ohm's law. The applied voltage (reference signal) is divided by the corresponding current generated by the unknown impedance (measured signal).

$$\frac{REFERNCE\_SIGNAL}{MEASURED\_SIGNAL} = \frac{Vout(\omega)}{Iin(\omega)} = Z(\omega) \quad (12)$$

Digital Fourier Transform (DFT) is performed on the ADC data and the real and imaginary components of the impedance measured are stored in the chip data registers. The magnitude and phase of the measured impedance is calculated by:

$$\text{Magnitude} = \sqrt{R^2 + I^2} \quad (13)$$

$$\text{Phase} = \tan^{-1} (I/R) \quad (14)$$

Phase and magnitude values of impedance are transferred to computer for further processing. The final value of magnitude is multiplied by a gain factor. Before measuring any impedance, the AD5933 must be calibrated and the gain factor has to be calculated. The calibration and gain factor calculation is performed to compensate for errors caused by the device electronic components such as time delays, attenuation, etc. The calibration

and gain factor calculation is performed by connecting and measuring known impedance between $V_{IN}$ and $V_{OUT}$. The impedance magnitude is measured by the device and the gain factor is calculated by using the following formula:

$$Gian\_Factor = \frac{\frac{1}{KNOWN\_IMPEDANCE}}{CALCULATED\_MAGNITUDE} \quad (15)$$

Finally, the value of the unknown impedance magnitude under measurement is calculated according to the following equation:

$$UNKNOWN\_IMPEDANCE = \frac{1}{CALCULATED\_MAGNITUDE \times Gian\_Factor} \quad (16)$$

The AD5933 desktop software is used to calculate the gain factor and the final value of magnitude. The real and imaginary values from the data register are transferred to the software and processed to acquire the final results. The software and communication protocol between the computer and chipset is $I^2C$ which will be discussed in the next sections of this chapter.

### 4.1.4 Experimental result

To check the functionality of the device, CultureWare electrodes from Applied Biophysics Inc. were used. Array Configuration used is shown in Figure 26. It can be observed from Figure 27, that the impedance measured for 100kΩ resistance is less actual value. It is measured at 80kΩ. This is due to device calibration issues; however, the results show the transition steps and continuous time measurement functionality.

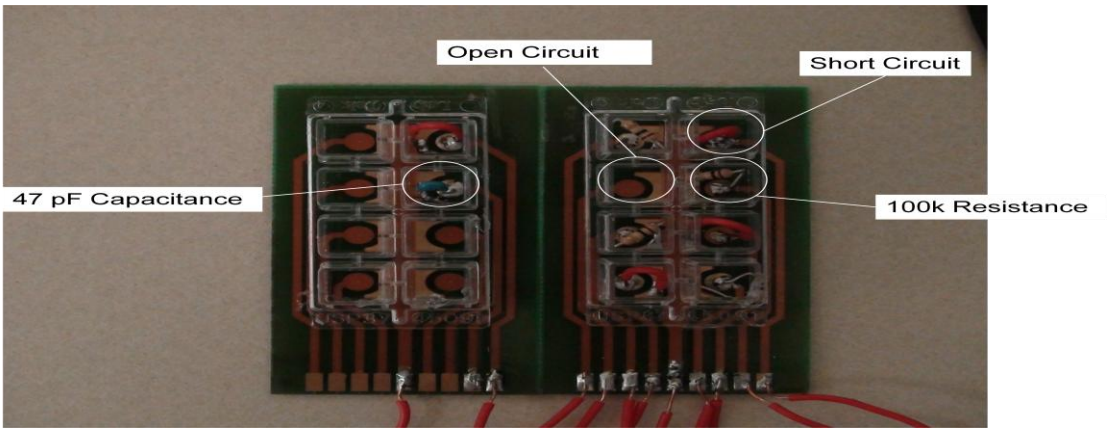


**Figure 26:** Electrode arrays

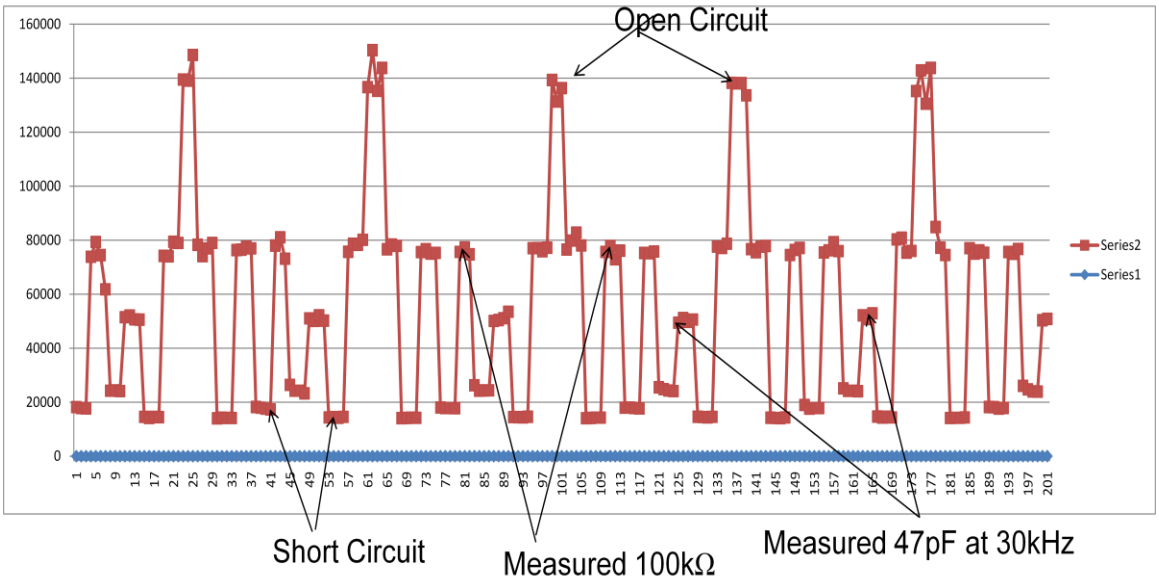


**Figure 27:** Experimental test of electrode array

## 4.2 Programming

In this section, an overview of $I^2C$ is provided, and the communication links from the chipset to the user interface are presented. A description of the original software and logarithms used by the AD9533 also are described and our modifications on both the algorithm and graphic user interface (GUI) are demonstrated.

### 4.2.1 Principle

Analog devices chipset package contains a single PCB and a Compact Disc (CD) is provided to install the interface software. USB port is used to connect the AD9533 Evaluation board to the computer. A computer is used to both program the device registers on the AD9533 chipset and acquire the impedance results. The communication protocol between the Computer and AD5333 Evaluation board is $I^2C$. $I^2C$ is a half-duplex system in which it cannot send and receive at the same time. It has two bi-directional lines Serial Clock (SCL) and Serial Data (SDA) to communicate with the connected device. The on-board microcontroller is programmed via a visual basic (GUI) program to control and acquire data from the chipset. The communication links are shown in Figure 28.

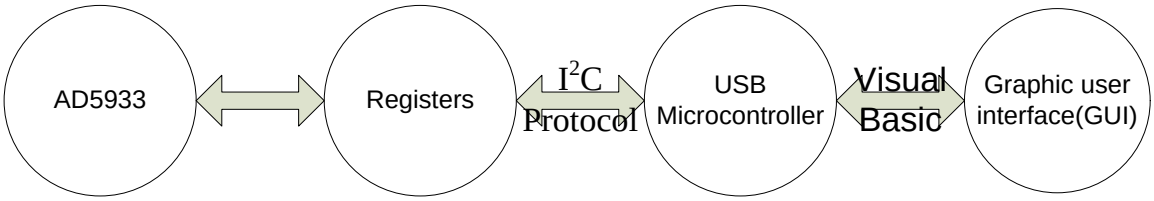


**Figure 28:** Analog Devices communication protocols

Beside the pre-complied executable program that comes with the CD, Analog Devices has provided the software source code that can be complied. There are chipset registers that are written and read through the program. The software modifications are done by programming the registers and modifying the software configurations. The original GUI interface is shown in Figure 29. The algorithm used by Analog Devices software is presented in Figure 30.

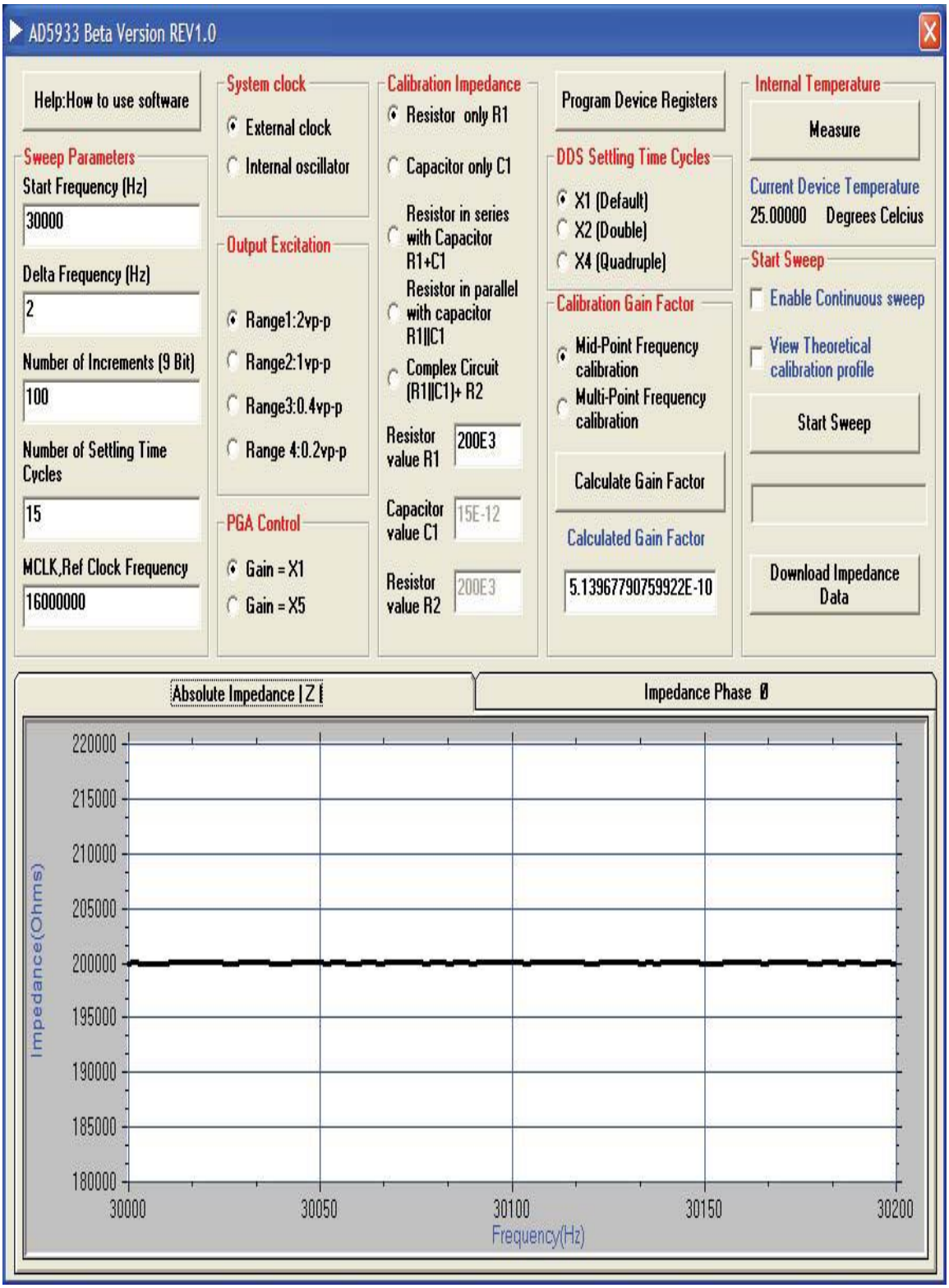


**Figure29:** Original GUI

### 4.2.2 Algorithms

The software is designed for frequency sweep analysis of a single target. After the sweep is complete a graph of impedance vs Frequency and Phase vs frequency is displayed in the GUI. A single frequency sweep flow chart is presented in Figure 30.

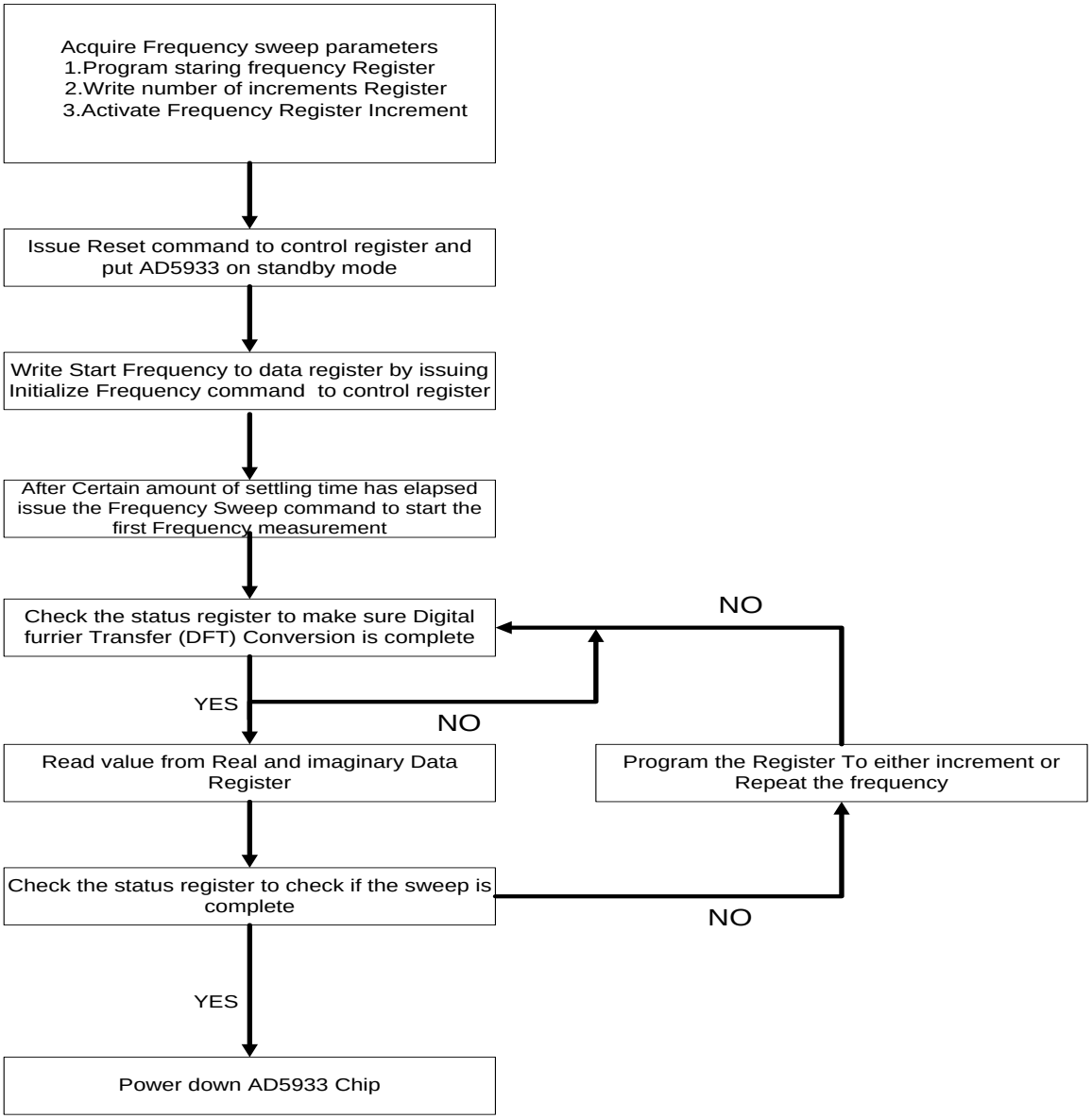


**Figure 30:** Original software algorithm

### 4.2.3 Software modifications

The chipset AD5933 is programmed and controlled by a set of registers. The register addresses go from 0x80 to 0x97. The control registers are from 0x80 to 0x81 and are used for the modifications:

| D15 | D14 | D13 | D12 | Function |
|---|---|---|---|---|
| 0 | 0 | 0 | 0 | No operation |
| 0 | 0 | 0 | 1 | Initialize Start Frequency |
| 0 | 0 | 1 | 0 | Start Frequency Sweep |
| 0 | 0 | 1 | 1 | Increment Frequency |
| 1 | 0 | 0 | 1 | Repeat Frequency |
| 1 | 1 | 0 | 1 | Measure Temperature |
| 0 | 1 | 1 | 0 | Power-down mode |
| 0 | 1 | 1 | 1 | Standby mode |

**Table 2:** An analog device programmable registers

The original software includes the options for Single sweep and Continuous sweep. In single sweep a start frequency and frequency increment is set and at each frequency the impedance is measured and stored in a .CSV format file which can be opened by a Microsoft Excel™ spreadsheet. In continuous sweep, the sweep will continue in a loop until the user stops the sweep. The sweep program will only save the last loop of data and each loop takes about 1 to 2 seconds to execute. There are no options to set the sampling rate period and the number of samples is directly proportional to the number of frequency increments. For biological impedance monitoring applications and the study of their behaviors, having the ability to see how interactions between materials change the impedance over-time is essential. This is important for continuous glucose monitoring since the changes are over-time and protein reactions take time to completely stabilize.

In order to study what happens during this period the original program needs to be modified to have a specific sampling rate and store the entire results for further analysis.

Single sweep function is a subroutine block in the visual basic program that has been modified. This subroutine handles Single sweep in the visual basic program and is named Private Sub Sweep_single() . The subroutine code blocks extracts with comments are as, follow:

Sweep_single():

Declare Variables:

```
Dim Impedance As Double
```

Setup $I^2C$ communication protocol: $I^2C$ protocol is initialized by calling the corresponding subroutines:

```
Public Function PortWrite( DeviceAddress As Long, AddrPtr As Long, DataOut As Long) As Integer
```

Acquire Time interval and number of sample (increment) and frequency and write the value to the corresponding register and power up the device:

```
WritetToPart &H84, StartFrequencybyte0 '84 hex lsb
WritetToPart &H83, StartFrequencybyte1 '83 hex
WritetToPart &H82, StartFrequencybyte2 '82 hex
EnterStandbyMode                    ‘put the AD5933/34 into standby mode, all internal circuitry powered up
 UpdateStartFrequency
 UpdateNumberIncrement
 UpdateFrequencyIncrement
```

Initialize single sweep:

```
Do While ((Increment <> 0))
Calculate the impedance and check if the device is working correctly
Increment = Increment - 1 ' number of increments of sweep at the start and dcrease each time a sweep is performed
Frequency = Frequency + Frequency Increments '  increase the frequency
Wait( time )  #1
```

```
Repeat the frequency    #1
Loop until the frequency sweep is complete
```

In the last part of the code the device is put into standby mode and the sweep is initiated. The sweep is set on a loop frequency and is incremented after each loop and impedance calculation is completed; however, for this project a measurement of impedance over a time interval is required. To achieve the time sweep, UpdateFrequencyIncrement is removed from the single sweep subroutine and following subroutines are added:

```
Private Declare Sub Sleep Lib "Kernel32.dll" (ByVal dwMilliseconds As Long)
Private Declare Function timeGetTime Lib "WinMM.dll" () As Long
```

The subroutine wait is added to the code. The time between each sample is acquired from the user. Each time a single sweep loop is performed the functions “wait (time)” and “repeat frequency” are called which makes the device wait for specified time and then repeat the same frequency sweep again.

The arrays are updated each time a measurement is taken. The arrays are used to constantly update the real-time graph incorporated in the software. Each time a new value is measured the graph is refreshed so that what user sees a continuous graph of time versus impedance. Finally, to store the results in an Excel format the following coding is used:

```
For count = 0 To (NumberIncrements)
    GlobalDataArray1(count) = RealDataArray(count)
    GlobalDataArray2(count) = ImagineryDataArray(count)
    GlobalDataArray3(count) = MagnitudeArray(count)
    GlobalDataArray4(count) = PhaseArray(count)
    GlobalDataArray5(count) = code(count)
```

```
    Print #iFB_TMP06, (Timearray(count)); (","); (GlobalDataArray3(count)); (","); (GlobalDataArray4(count)); (",");
(GlobalDataArray1(count)); (","); (GlobalDataArray2(count)); (","); (GlobalDataArray5(count))
    'Next count
    Next count
  Close #iFB_TMP06
Exit Sub
```

The format of the file includes time, frequency, real and imaginary values and impedance

The flow chart of the code and the modification indicated in blue are shown in Figure 31.

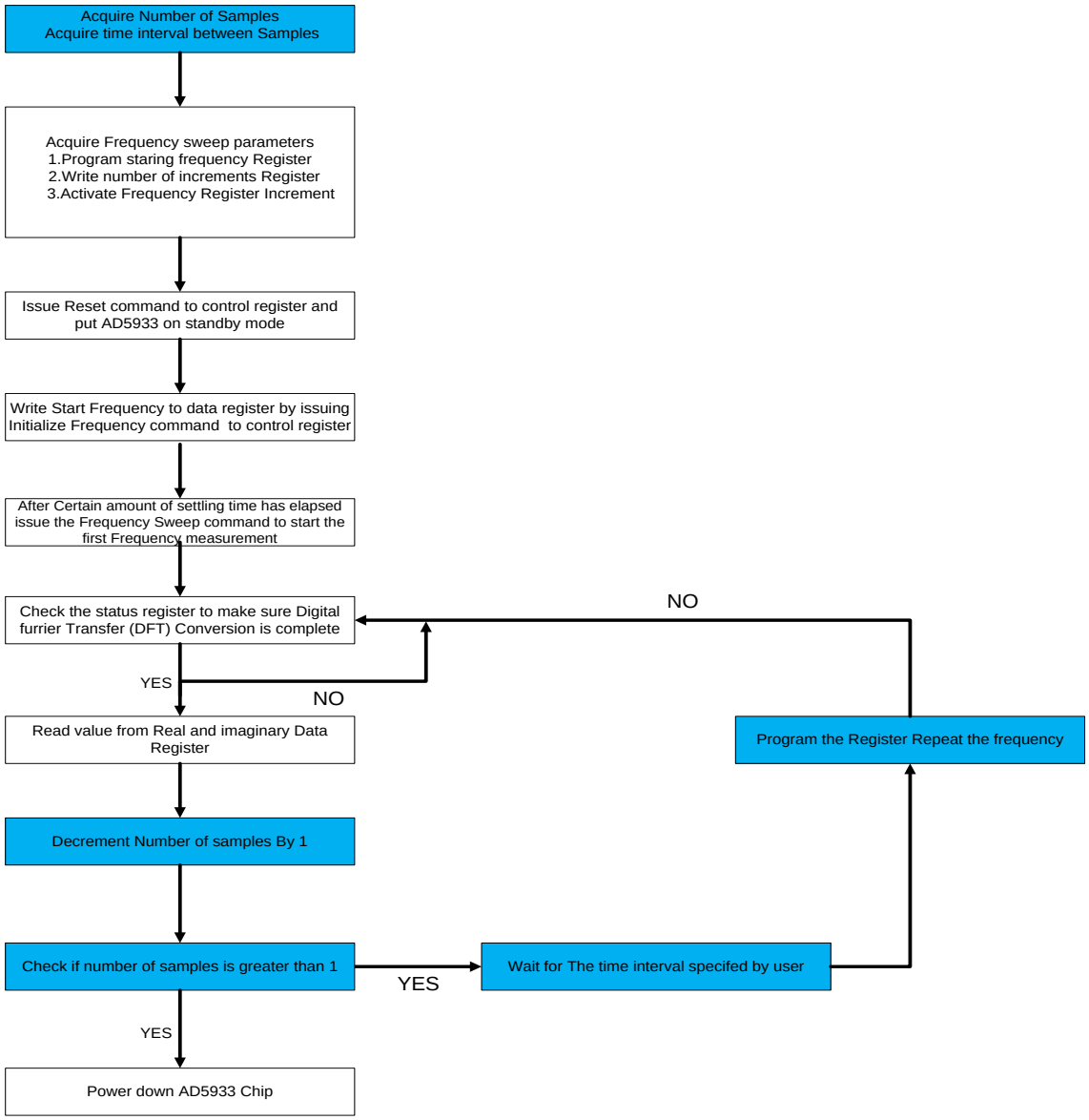


**Figure 31:** Modified Software Algorithm

Since the applet that displays the graphical results used by this software is a third party software, another graph drawing software has been embedded in the system software. The modifications to the interface are shown Figure 32.

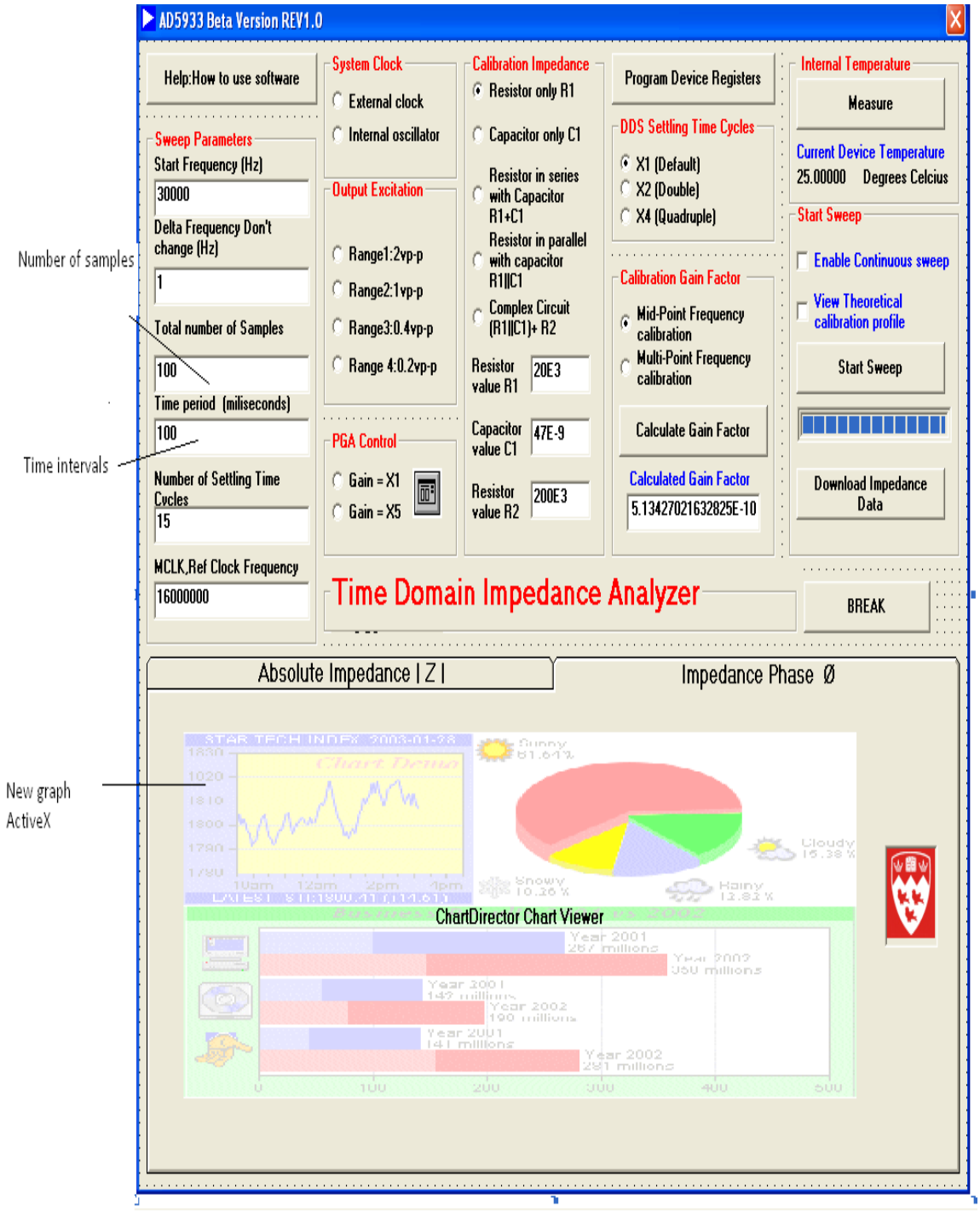


**Figure 32:** Modified GUI

The time interval is in milliseconds and after each interval the graph will be updated so the user can see a continuous impedance spectroscopy graph. The total time a sample could be monitored is dependent on the number of samples and the time interval. For example, if a sample needs to be monitored for 30 min then setting could be set to 360 samples each taken every 5 second interval.

The program modification could also enable this device to change the frequency while making time based measurement. The register can be programmed in such way to increase the frequency after a certain amount of time has elapsed during the measurement. This will result a graph with both time and frequency as variable. Although there are many modifications that can be made to suit various applications for this device,the current modifications are more than suffice for the glucose sensing.

# CHAPTER 5

## Biological Testing results

### 5. Overview Biological Testing results

In this section, we provide a test setup for the prototype glucose sensor. Different concentrations of glucose were applied to the sensing electrodes and the impedance change resulting from concentration was measured. From this measurement, a profile is created to detect each concentration. Test tubes with different glucose concentration were used and the concentrations were measured in sequence by immersing the sensing electrodes into the test tubes. The impedance changes corresponding to each concentration was then measured. In this section, the measurements in frequency-domain, and then in time-domain are demonstrated.

### 5.1 Frequency-domain measurements

After exposing the sensing electrodes to each glucose concentration, the device was programmed to sweep the frequency from 25 kHz to 100 kHz. The impedance variation in this range frequency was measured and recorded. The resulting graph is shown in Figure 33. It can be observed that at higher glucose concentrations, the higher impedance variations were obtained. At low frequencies, the impedance had a higher value for each concentration and as frequency is increased the value of impedance decreased..

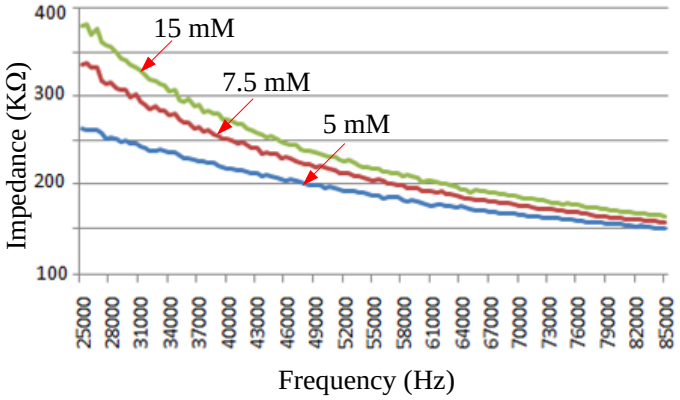


**Figure.33:** Frequency sweep of different concentration of glucose

### 5.2 Time-domain measurements

For time-domain measurements electrode was rapidly removed from a testing tube and immersed in another one. Figure 34 shows the impedance variations for different concentrations (0.5mM, 1mM, 2.5mM, 5mM, and 7.5mM).

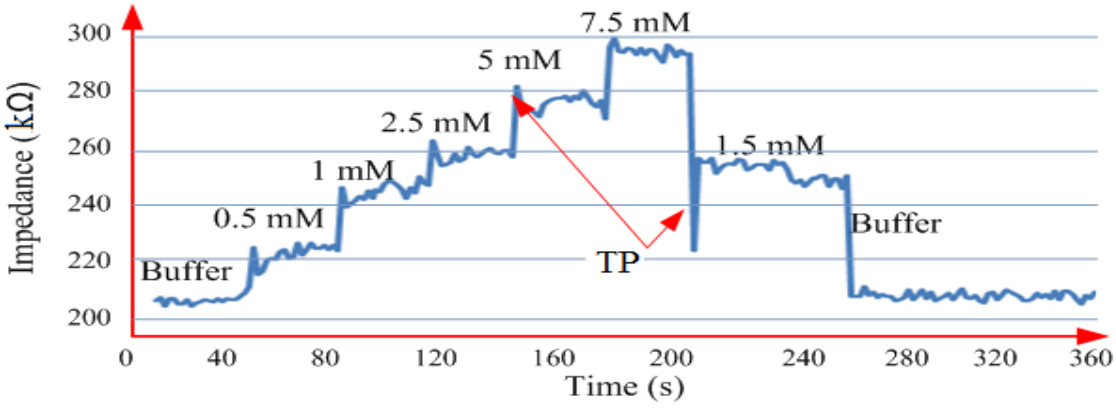


**Figure.34:** Impedance Change of Bio-sensing electrode impedance

It can be observed that this protein based biosensor was sensitive to glucose concentrations in the physiologically relevant range from 0.5 mM to 7.5mm . The spikes in the results were due to removing the electrode from one concentration tube to another.

In the actual measurements these spikes will not happen as the electrode will be subjected to continuous sample flow.

The following test was performed to confirm that tests were repeatable. In this test the sensing electrode was immersed in a glucose concentration and then removed and was inserted in the buffer solution. The electrode was immersed in the same glucose concentration again. It can be observed from Figure 35 after the electrode was exposed to the solution again the impedance returned to the same value.

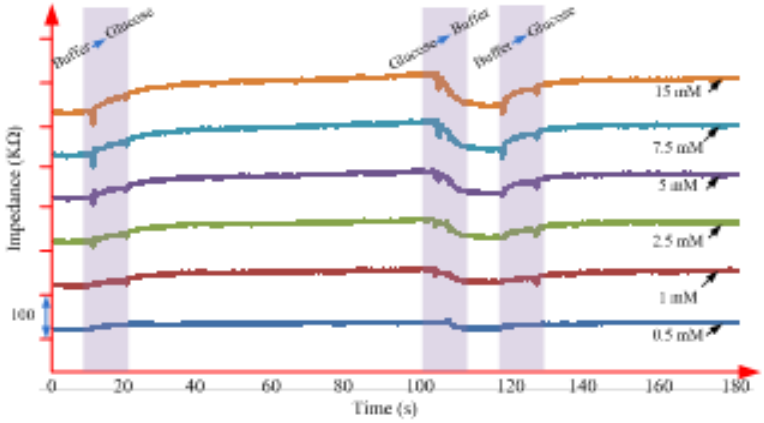


**Figure.35:** Repeatable tests

In this section impedance measurements of different concentration of glucose using a regent-less protein based biosensor was obtained. Preliminary results demonstrate the viability for continuous glucose monitoring using protein based biosensor and microfabricated electrodes. However, further testing and calibration of device should be performed to make it viable for clinical and medical applications.

## 6. Conclusion and Future Works

In this thesis a portable impedance measurement system was presented. The system was tested using different glucose concentrations to prove the sensor system functionality. The contributions of thesis are: (i) design and fabrication of inter-digitized electrode suitable for biosensor applications, (ii) collaborate with the Mark Trifiro's research group at the Lady Davis Institute for Medical research to develop engineered proteinaceous glucose receptors (Glucokinase molecules) and proper linker chemistry to immobilize glucokinase molecules on gold metal electrodes, (iii) modification of the impedance measurement device, both the hardware and software, for continuous time electrochemical impedance spectroscopy and (iv) perform measurement of glucose concentration in continuous time with the developed sensing electrode. The knowledge acquired in this research can be translated to other chronic diseases such as high cholesterol and cardiovascular diseases. The ultimate goal of the project is to develop an implantable glucose biosensor. It is still a long way from achievement, but the demonstrate system will serve as a first prototype which will help us in developing single-chip microsensors using CMOS integrated circuit.

REFERENCES


1. Hierlemann, A. (2005). Integrated Chemical Microsensor Systems in CMOS Technology (Microtechnology and MEMS)
2. Zhang Y , W. Y., Wang H, Jiang J , Shen G, Yu R, Li J (2009). "Electrochemical DNA Biosensor Based on the Proximity-Dependent Surface Hybridization Assay." Analytical Chemistry 81(5): 1982-1
3. Blanes L , M. M., Do Lago C, Ayon A , Garcia C (2007). "Lab-on-a-chip biosensor for glucose based on a packed immobilized enzyme reactor." Electroanalysis 19(23): 2451-2456.
4. Arya S, . Datta M , Malhotra B (2008). "Recent advances in cholesterol biosensor." Biosensors & Bioelectronics 23(7): 1083-1100.
5. Cortina M, E. M., Alegret S , del Valle M (2006). "Urea impedimetric biosensor based on polymer degradation onto interdigitated electrodes."Sensors and Actuators B Chemical 118(1-2): 84-89.
6. Sun N, L. Y., Lee H , Weissleder R , Ham D (2009). "CMOS RF Biosensor Utilizing Nuclear Magnetic Resonance." IEEE Journal of Solid-State Circuits 44(5): 1629-1643.
7. Bogue, R. (2007). "Optical chemical sensors for industrial applications." Sensor Review 27(2): 86-90.
8. Newman, J. D. and S. J. Setford (2006). "Enzymatic biosensors." Molecular Biotechnology 32(3): 249-268.
9. Zhu, P. X., D. R. Shelton, et al. (2005). "Detection of water-borne E-coli O157 using the integrating waveguide biosensor." Biosensors & Bioelectronics 21(4): 678-683.

10. Yao, C. Y., T. Y. Zhu, et al. (2008). "Hybridization assay of hepatitis B virus by QCM peptide nucleic acid biosensor." Biosensors & Bioelectronics 23(6): 879-885.
11. Ko, S. H. and S. A. Grant (2006). "A novel FRET-based optical fiber biosensor for rapid detection of Salmonella typhimurium." Biosensors & Bioelectronics 21(7): 1283-1290.
12. Kim, Y. H., J. S. Park, et al. (2009). "An impedimetric biosensor for real-time monitoring of bacterial growth in a microbial fermentor." Sensors and Actuators B Chemical 138(1): 270-277
13. Berggren, C., B. Bjarnason, et al. (2001). "Capacitive biosensors." Electroanalysis 13(3): 173-180.
14. Berggren, C., P. Stalhandske, et al. (1999). "A feasibility study of a capacitive biosensor for direct detection of DNA hybridization." Electroanalysis 11(3): 156-160.
15. Lin, S. X. and K. E. Neet (1990). " Demonstration of a Slow Conformational Change in Liver Glucokinase by Fluorescence Spectroscopy " Journal of Biological Chemistry 265(17): 9670-9675.
16. Haab, B. B. (2003). "Methods and applications of antibody microarrays in cancer research." Proteomics 3(11): 2116-2122.
17. Olkhov, R. V. and A. M. Shaw (2008). "Label-free antibody-antigen binding detection by optical sensor array based on surface-synthesized gold nanoparticles." Biosensors & Bioelectronics 23(8): 1298-1302.
18. Banada, P. P., S. L. Guo, et al. (2007). "Optical forward-scattering for detection of Listeria monocytogenes and other Listeria species." Biosensors & Bioelectronics 22(8): 1664-1671.

19. Chodavarapu, V. P., D. O. Shubin, et al. (2007). “CMOS-based phase fluorometric oxygen sensor system”, IEEE Transactions on Circuits and Systems 54(1): 111-118
20. Ho, H. P., W. C. Law, et al. (2005). “Real-time optical biosensor based on differential phase measurement of surface plasmon resonance” Biosensors & Bioelectronics 20(10): 2177-2180
21. Xie, B. and B. Danielsson (1996). "An integrated thermal biosensor array for multianalyte determination demonstrated with glucose, urea and penicillin." Analytical Letters 29(11): 1921-1932.
22. Chemla, Y. R., H. L. Crossman, et al. (2000). "Ultrasensitive magnetic biosensor for homogeneous immunoassay." Proceedings of the National Academy of Sciences of the United States of America 97(26): 14268-14272
23. Lee, H., Y. Liu, et al. (2006). "IC/Microfluidic hybrid system for magnetic manipulation of biological cells." IEEE Journal of Solid-State Circuits 41(6): 1471-1480.
24. Daniels, J. S. and N. Pourmand (2007). "Label-free impedance biosensors: Opportunities and challenges." Electroanalysis 19(12): 1239-1257
25. Berggren, C. and G. Johansson (1997). "Capacitance measurements of antibody-antigen interactions in a flow system." Analytical Chemistry 69(18): 3651-3657
26. Ong, K. G., J. Wang, et al. (2001). "Monitoring of bacteria growth using a wireless, remote query resonant-circuit sensor: application to environmental sensing." Biosensors & Bioelectronics 16(4-5): 305-312

27. Khanna, V. K., A. Kumar, et al. (2006). "Design and development of a novel high-transconductance pH-ISFET (ion-sensitive field-effect transistor)-based glucose biosensor." International Journal of Electronics 93(2): 81-96

28. Kristensen, G. B. B., K. Nerhus, et al. (2004). "Standardized evaluation of instruments for self-monitoring of blood glucose by patients and a technologist." Clinical Chemistry 50(6): 1068-1071

29. Pinget, M., N. Jeandidier, et al. (1995). "Multicenter trial of programmable implantable insulin pump in type ! diabetes." International Journal of Artificial Organs 18(6): 322-325

30. alimi, A., E. Sharifi, et al. (2007). "Immobilization of glucose oxidase on electrodeposited nickel oxide nanoparticles: Direct electron transfer and electrocatalytic activity." Biosensors & Bioelectronics 22(12): 3146-3153

31. Bankar, S. B., M. V. Bule, et al. (2009). "Glucose oxidase - An overview." Biotechnology Advances 27(4): 489-501

32. Wang, J. (2001). "Glucose biosensors: 40 years of advances and challenges." Electroanalysis 13(12): 983-988

33. Guilbaul.Gg and G. J. Lubrano (1973). " An enzyme electrode for the amperometric determination of glucose." Analytica Chimica Acta 64(3): 439-455

34. Aoki, K., H. Suzuki, et al. (2005). “Thermophilic glucokinase-based sensors for the detection of various saccharides and glycosides” 108(1-2): 727-732

35. D'Auria, S., N. DiCesare, et al. (2002). "A novel fluorescence competitive assay for glucose determinations by using a thermostable glucokinase from the thermophilic

microorganism Bacillus stearothermophilus." Analytical Biochemistry 303(2): 138-144.

36. Rose Lumbroso, Nassima Naas (2007)"Novel Bioimpedance Sensor for Glucose Recognition " Signals, Systems and Electronics, pages:41-43
37. A. Trifiro "Glucose sensor and uses thereof" US patent, 0232370 A1, 2003.
38. Li, A. X., F. Yang, et al. (2007). "Electrochemical impedance detection of DNA hybridization based on dendrimer modified electrode." Biosensors & Bioelectronics 22(8): 1716-1722
39. Cho, S., S. Becker, et al. (2007). "Impedance monitoring of herpes simplex virus-induced cytopathic effect in Vero cells." Sensors and Actuators B Chemical 123(2): 978-982
40. Rahman, A. R., G. Justin, et al. (2009). "Towards an implantable biochip for glucose and lactate monitoring using microdisc electrode arrays (MDEAs)." Biomedical Microdevices 11(1): 75-85.
41. www.biophysics.com
42. Van Gerwen, P., W. Laureyn, et al. (1998). "Nanoscaled interdigitated electrode arrays for biochemical sensors" Sensors and Actuators B Chemical 49(2): 73-80
43. Steinschaden, A., D. Adamovic, et al. (1997). "Miniaturised thin film conductometric biosensors with high dynamic range and high sensitivity" Sensors and Actuators B Chemical 44(1-3): 365-369
44. Zou, Z. W., J. H. Kai, et al. (2007). "Functionalized nano interdigitated electrodes arrays on polymer with integrated microfluidics for direct bio-affinity sensing using impedimetric measurement" Sensors and Actuators A Physical 136(2): 518-526

45. M. Abramowitz, I.A. Stegun,(1970)" Handbook of Mathematical Functions" pp. 589–607

46. Marrakchi, M., C. Martelet, et al. (2007). "An enzyme biosensor based on gold interdigitated thin film electrodes for water quality control." Analytical Letters 40(7): 1307-1316

47. Evgenij Barsoukov , R. M. (2005). Impedance Spectroscopy: Theory, Experiment, and Applications, Wiley-Interscience.

48. Jia, J. Y., W. J. Guan, et al. (2008). "Carbon nanotubes based glucose needle-type biosensor." Sensors 8(3): 1712-1718

49. Yan, W., X. M. Feng, et al. (2008). "A selective dopamine biosensor based on AgCl@polyaniline core-shell nanocomposites." Bioelectrochemistry 72(1): 21-27

50. Ghafar-Zadeh, E., M. Sawan, et al. (2007). "Novel direct-write CMOS-based laboratory-on-chip: Design, assembly and experimental results." Sensors and Actuators A Physical 134(1): 27-36

51. Kamata, K., M. Mitsuya, et al. (2004). "Structural basis for allosteric regulation of the monomeric allosteric enzyme human glucokinase." Structure 12(3): 429-438

52. T. McKee , J. R. M. (1999). Biochemistry: An Introduction, McGraw-Hill Education.

53. Marquette, C. A., M. F. Lawrence, et al. (2006). "DNA covalent immobilization onto screen-printed electrode networks for direct label-free hybridization detection of p53 sequences." Analytical Chemistry 78(3): 959-964

54. Kao, M. (2007). The study of impedance spectroscopy for single cell analysis <http://etdncku.lib.ncku.edu.tw/ETD-db/ETD-search/view_etd?URN=etd-0820107-

143736>". Department of Electrical Engineering, National Cheng Kung University. Master's Electrical Engineering